Pergamon

Geochimica et Cosmochimica Acta, Vol. 60, No. 23, pp. 4831–4852, 1996

0016-7037/96 $15.00 + .00

PII S0016-7037(96)00245-1

Natural fission reactors in the Franceville basin, Gabon: A review of the conditions and results of a "critical event" in a geologic system

F. GAUTHIER-LAFAYE,[1] P. HOLLIGER,[2] and P.-L. BLANC[3]

[1]Centre de Géochimie de la Surface, CNRS, 1 rue Blessig, 67084 Strasbourg Cedex, France
[2]Commissariat à l'Energie Atomique, CEA-Cadarache, BP 13108, Saint-Paul-les-Durance, France
[3]Institut de Protection et de Sûreté Nucléaire, CEA-FAR, BP 6, 92265 Fontenay-aux-Roses, France

(*Received December* 1, 1995; *accepted in revised form July* 2, 1996)

Abstract—Natural nuclear fission reactors are only known in two uranium deposits in the world, the Oklo and Bangombé deposits of the Franceville basin: Gabon. Since 1982, five new reactor zones have been discovered in these deposits and studied since 1989 in a cooperative European program. New geological, mineralogical, and geochemical studies have been carried out in order to understand the behavior of the actinides and fission products which have been stored in a geological environment for more than 2.0 Ga years. The Franceville basin and the uranium deposits remained geologically stable over a long period of time. Therefore, the sites of Oklo and Bangombé are well preserved. For the reactors, two main periods of actinide and radionuclides migration have been observed: during the criticality, under *P-T* conditions of 300 bars and 400–500°C, respectively, and during a distention event which affected the Franceville basin 800 to 900 Ma ago and which was responsible for the intrusion of dolerite dikes close to the reactors. New isotopic analyses on uranium dioxides, clays, and phosphates allow us to determine their respective importance for the retention of fission products. The UO_2 matrix appears to be efficient at retaining most actinides and fission products such as REEs, Y, and Zr but not the volatile fission products (Cd, Cs, Xe, and Kr) nor Rb, Sr, and Ba. Some fissiogenic elements such as Mo, Tc, Ru, Rh, Pd, and Te could have formed metallic and oxide inclusion in the UO_2 matrix which are similar to those observed in artificial spent fuel. Clays and phosphate minerals also appear to have played a role in the retention of fissiogenic REEs and also of Pu.

1. INTRODUCTION

Natural fission reactors are very high grade uranium ores where chain fission reactions occurred 2.0 b.y. ago (Bodu et al., 1972; Neuilly et al., 1972). At present time, the remains of the only reactors known in the world are located in two uranium ore deposits of the palaeoproterozoic Franceville basin, Gabon, namely Oklo and Bangombé.

During the seventies, the Oklo natural fission reactors were studied in detail mainly for their physical and neutronic interests (Naudet, 1975; Reuss, 1975; Brookins, 1975; Naudet, 1976, 1978). At Oklo, fission reactions occurred in an ore having enriched ^{235}U ($^{235}U/^{238}U$ = 3.7%). The main neutronic parameters have been precisely determined and the distribution of the end-member fission products and actinides are in good agreement to what can be expected from such reactors (Naudet and Renson, 1975; Neuilly and Naudet, 1975; Ruffenach, 1978). This led to the conclusion that the reactors can be considered as a closed-system for actinides and some fission products since the last chain fission reactions. The reason which were invoked for this closed-system behavior was that the uraninite crystals in which fission reactions occurred. They could retain the actinides and the fission products having ionic radii similar to that of uranium.

In the early 1980s there was renewed interest in the Oklo reactors, as they provided a unique opportunity to study actinide and fission product migration in a natural system of great age. It appeared at that time that very little data was available on the various solid phases of the reactors. In particular, no chemical analyses of uraninite crystals were published and almost nothing was known on mineral phases such as clays and phosphates and on the organic matter which forms an important phase in the reactors.

In 1990, a new program was initiated as a European Community project "Oklo: Natural analogue." These studies attempted to reconstruct the geological history of the reactors, to determine the physical conditions of the fission reactions and to decipher the behavior of the actinides and fission products in the various rocks surrounding the reactors. Particular attention has been paid to the behavior of organic phases (Nagy et al., 1991, 1993) and various minerals such as clays, apatites, sulfides towards the containment of actinides, and fission products. The aim of this paper is to summarize the main results obtained on these mineral phases during these last five years on the so called "new reactors."

2. GEOLOGICAL BACKGROUND

The Franceville basin which hosts the uranium deposits of Gabon lies unconformably on the crystalline Archean basement of North Gabon and Chaillu. The Francevillian series is a sedimentary series of Palaeoproterozoic age which has been first described by Weber (1968). This series is divided into five units indicated as the FA basal formation to the FE formation at the top. The FA formation is composed of fluviatile and deltaic conglomerates and sandstones ranging in thickness from 100 m close to the edges of the basin to more than 1000 m in the subsiding areas. All uranium deposits are located in this FA formation. At Oklo and Bangombé, the uranium mineralization occurs in the uppermost layers at the top of the FA

formation. These sediments correspond to tidal bars of medium-sized sandstones with lateral extensions of more than one kilometer. The FA formation is overlain by FB black shales with thickness ranging from 400 m at the edges of the basin to more than 1000 m in the central parts of the basin. At the edges of the basin, dolomites, sandstones, and sedimentary breccias (olistholites) are interbedded in this FB formation. The FC to FE formations are mainly volcano-sedimentary, with some intercalations of jaspers and dolomites.

The Franceville basin is affected by dolerite intrusions which form a very dense E-W network of 5 to 20 m thick dikes. These dikes are typically 1 to 3 km apart and are linked to a major N-S dolerite intrusion with a thickness of up to 50 meters (Fig. 1).

One of the particularities of the Franceville series is the fact that in spite of its Palaeoproterozoic age it has never been severely metamorphosed which is almost certainly the reason why the reactors in the basin have been well preserved. The highest diagenetic level reached by the sediments corresponds to the level defined by Winkler (1976) as very low grade metamorphism characterized by crystallization of chlorite and illite, mainly of 1 M polytype (Gauthier-Lafaye, 1986). Only at the bottom of the FA formation, 2 M-illite may have some importance. Fluid inclusion studies of quartz overgrowths and carbonate cements indicate that the maximum temperature reached in the Franceville basin during diagenesis ranges between 180 and 200°C at a pressure of 400 bars (Openshaw et al., 1978; Gauthier-Lafaye and Weber, 1981, 1989; Savary and Pagel, 1993). During burial the sediments reached the oil window and maturation of syngenetic organic matter led to the formation of liquid hydrocarbons (Vanderbrouck et al., 1978; Cortial et al., 1990). The FB black shales were the main source rock for hydrocarbons and the FA sandstones are the rock reservoir for such liquid bitumen (Gauthier-Lafaye and Weber, 1981; Cortial et al., 1990). Sm-Nd data obtained on clay minerals which crystallized when petroleum was mobile suggest that maturation and migration of hydrocarbons occurred soon after deposition of the sediments, during the early diagenesis (Stille et al., 1993).

The Francevillian series has been dated by several geochronometers. Rb-Sr and K-Ar data on volcanic rocks interbedded within the FB formation yielded an age of 2143 ± 143 Ma (Bonhomme et al., 1982) which represents the age of sediment deposition. Similar ages of 2099 ± 115 Ma and 2036 ± 79 Ma (Bros et al., 1992) have been found with two Sm-Nd isochrons on small authigenic clay fractions of the FB formation which are contemporaneous with the early diagenesis of the Francevillian sediments. K-Ar and Rb-Sr ages of 1843 ± 42 Ma and 1870 ± 78 Ma, respectively (Bonhomme et al., 1982), were also found on clays smaller than 2 μm of the FA and FB formations revealing a thermal event which reopened these isotopic systems. Overall K-Ar data on bulk rocks of a dolerite dike which cross-cut the Oklo open pit give very scattered ages ranging between 530 and 1000 Ma. However, two feldspathic fractions gave more precise ages of 977 and 981 ± 27 Ma which has been considered as the most probable age for the intrusion of this dike (Bonhomme et al., 1982). This dolerite intrusion corresponds to an important extensional event affecting the whole Franceville basin and during which fluids were mobilized into the basin. This event appears to have had an important influence on the behavior of uranium and fission products in the reactors.

The Franceville basin hosts six uranium ore deposits (Fig. 1) of different economic importance (Weber, 1968; Gauthier-Lafaye, 1986; Gauthier-Lafaye and Weber, 1989). The four most important deposits are located on the northwestern edge of the Franceville basin, along the eastern boundary of the Mounana basement horst. From north to south these are the deposits of Boyindzi and Mounana which are now mined out and the deposits of Oklo and Okelobondo which are in fact interconnected and presently producing mines. Oklo was first mined as an open pit where the first natural fission reactors (reactors 1 to 9) were found and is now, together with Okelobondo, mined underground. Uranium mineralization occurs in the upper part of the FA sandstones. The thickness of the mineralized layer mainly depends on the tectonic structures affecting the FA sandstones. At Mounana the deformation is intense and uranium is enclosed in a 100 meters deep vertical lens which develops at the intersection between N-S and WW-SE faults. At Oklo and Okelobondo, mineralization occurs in 5 to 8 m thick sandstones which are directly overlain by the organic carbon rich FB black shales. The main structure is a wide monoclinal fold giving a general dip of the layer to the east. Locally, secondary folds intersect this structure and are usually enriched in uranium. The two other deposits, namely Bangombé and Mikouloungou are located in more central parts of the basin. At Bangombé, uranium mineralization also occurs in the upper part of the FA sandstones and is located at the top of a wide anticline. The mineralized layer is only 10 to 30 m deep and has not been mined. In 1986, a new reactor was discovered there by drilling. At Mikouloungou the mineralization is associated with E-W normal fault which put the mineralized FA sandstone in tectonic contact with the FB black shales. Here, the uranium ores are located in the lower FA formation. All these uranium ore deposits are crossed

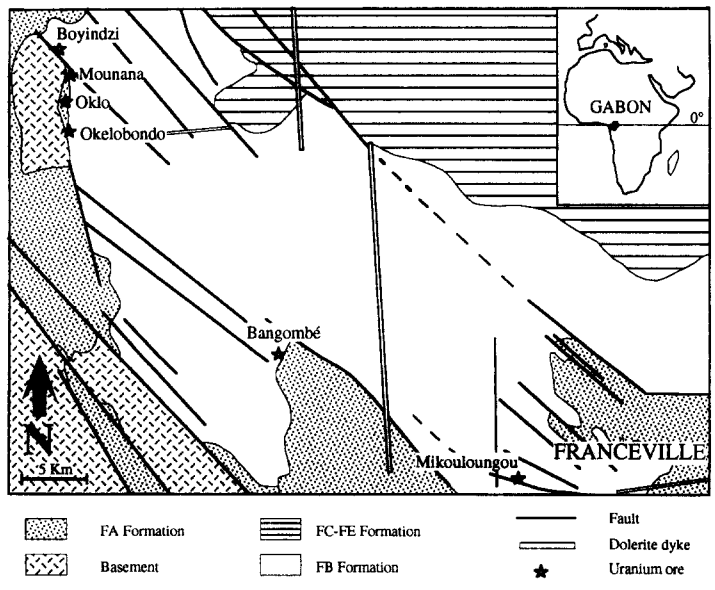

FIG. 1. Geological map of the Franceville basin.

by dolerite dikes. At Oklo, a 15 m wide E-W dike cuts across the FA and FB formations.

3. URANIUM MINERALIZATION AND INITIAL CONDITIONS OF THE FISSION REACTIONS

The uranium ore deposits of the Franceville basin are related to old petroleum traps and uranium mineralization occurred when oxidized bearing fluids met reducing conditions in the hydrocarbon accumulations (Gauthier-Lafaye, 1986; Gauthier-Lafaye and Weber, 1988, 1989). In the common ore of the deposits, uranium consists mainly of uraninite located in and around nodules of organic matter which fill the secondary porosity of the hosted sandstones. The uranium content of this ore range from 0.1 to 10%. At Oklo and at Bangombé, the mineralization is always associated with hydraulic fracturing. Such fracturing consists in a dense (10 to 100 μ) microfracture network which develops parallel to the bedding (Gauthier-Lafaye and Weber, 1988). These fractures are filled with calcite, organic matter, sulfides, and uranium. Hydraulic fracturing is mainly located where a drastic change of the sandstone grain size occurs from medium-sized sandstones to fine sandstones or pelites. The maximum uranium content always occurs in an area where hydraufracturing is well developed. This fracturing also affects the reactors and field relations have demonstrated that these fractures have been re-oriented as the result of the event responsible for the main tectonic structure of the deposit. This suggest that uranium mineralisation and the fission reactions occurred before the main tectonic event which has given to the Oklo deposit its present shape.

In areas affected by intense hydraufracturing resulting in brecciation of the rock, uranium content may reach values as high as 15%. In such cases, mineralization is closely related to oxidation-reduction fronts with the development of Fe-oxides. In the brecciated, oxidized ores, uranium forms 1 to 10 cm size irregular patches in the matrix and fills the microfracture networks. It is thought that fission reactions started in this type of ore when the uranium content reached the critical mass and the other conditions for chain fission were met. To model the criticality of the reactors, various parameters have to be taken into account such as the contents of B and REEs which are poison for neutrons and the content of U which allows it to reach the critical mass, the porosity of the sandstones which controls the amount of water (which acts as regulator of the fission reaction), the mineralogical composition of the ore (which controls the amount of elements having different cross section values) and the temperature which acts on the density of the water which is assumed to be the moderator for neutrons. Naudet (1991) has computed that at Oklo, the criticality could happen under two main conditions: (1) the mineralized sandstones must have been fractured in order to have an open porosity ranging between 10 and 15% and (2) fission reactions could start only in area having the highest uranium content ranging between 10 and 20%. Criticality was easily achieved in ore where sandstones had already lost some silica which at Oklo could have been in volume of around cubic meter of sandstone with a 10% uranium content.

When uranium mineralization occurred, hydrocarbons were still mobile and migrated into the secondary porosity, created by the hydrofracturing. Microthermometric data on fluid inclusions in calcites associated with uranium reveal that the temperature of the diagenetic fluids at the time of reactors operation range between 120 and 150°C under a pressure of 300 bars (Gauthier-Lafaye, 1986). Such temperatures are in good agreement with oxygen isotopic data obtained on diagenetic clay minerals related to the uranium ore and on calcites (Gauthier-Lafaye et al., 1989).

4. DESCRIPTION OF THE REACTORS

4.1. Physical Setting

The first reactors were discovered between 1972 and 1974 in the open pit of Oklo and were numbered 1 to 6 in the order of their discovery (Fig. 2). During the four years of the "Franceville" project these reactors were studied in great detail to ascertain the neutronic processes and the effects of the fission reactions on the rocks. Most of this work has been published in the proceedings of two meetings held in 1975 and 1977 in Libreville and Paris, respectively (The Oklo Phenomenon, IAEA, Vienna, 1975, and Natural Fission Reactors, IAEA, Vienna, 1978).

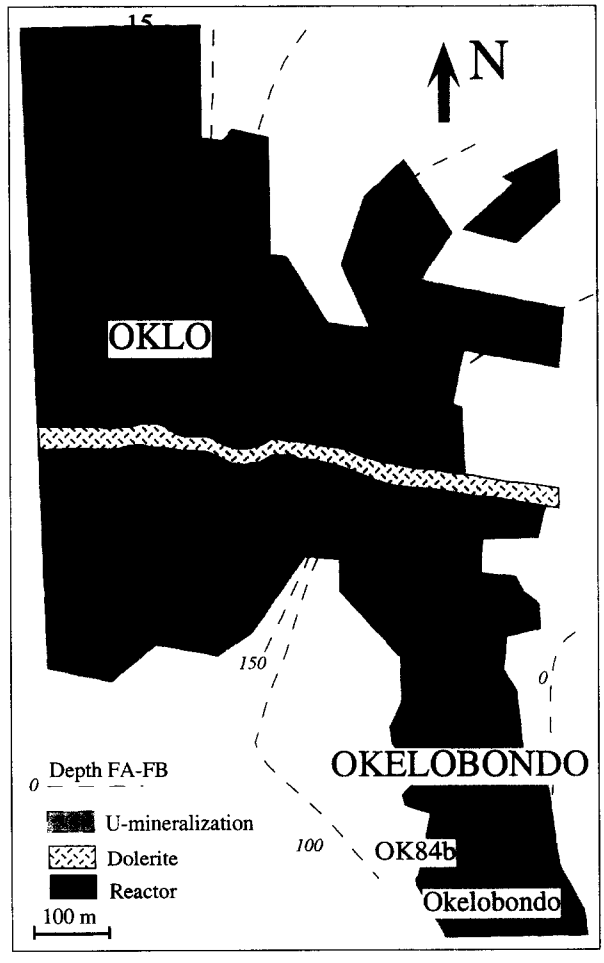

FIG. 2. Map of the Oklo deposit and location of the reactors.

In 1978, three other reactors numbered 7, 8, and 9 were discovered in the open pit of Oklo (Gauthier-Lafaye et al., 1979). These reactors differed significantly from zones 1–6 in three ways. The presence of high amount of organic matter, the low uranium content, and the lower ^{235}U depletion of the rocks where fission reactions occurred. However, and in spite of these important differences, these reactors were never studied in as much detail as the previous ones.

Since 1982, five other reactors, namely 10, 13, 16, OK84, and 15 or the so-called "Crochon" were discovered at Oklo and one at Bangombé 30 km south of Oklo. Reactors 10, 13, and 16 are located in the underground mine and were discovered during the mining of the East and South area of the Oklo deposit. The reactor OK84 which has only been recognized during drilling is located in the Okelobondo deposit which corresponds to the southernmost extension of the Oklo deposit. The reactor named Crochon is located in the northern part of the Oklo deposit and has been totally mined out. This reactor was never studied because its shape had been severely modified by locally complex tectonic structures. The reactor at Bangombé is very unusual in that it is located very near the surface (12 m deep) and has been affected by supergene weathering.

4.2. Reactor Operating Conditions

Natural fission reactors are characterized by an ore having abnormal uranium isotopic compositions (depletion in ^{235}U), containing fission products and endmember elements originating from short lived fission products. The remaining fissiogenic concentrations of most these elements in the core of the reactors is often in good agreement with the theoretical fission yield for ^{235}U, ^{238}U, Th, and ^{239}Pu (Shukolyukov et al., 1985; Hidaka et al., 1988; Hidaka and Masuda, 1988; Holliger, 1993, 1995; Hidaka, 1995).

Taking into account the isotopic composition and the contents of U, Th, and of the most stable fission products (mainly REEs but also Zr and Ru), it is possible to calculate the main neutronic parameters of the fission reaction. The calculated parameters are the fluence, the restitution factor of ^{239}Pu (ratio of the amount of ^{235}U produced by radioactive decay of ^{239}Pu and the amount of fissioned ^{235}U), the spectrum index (defined as the ratio between the capture cross section of the environment and its effectiveness at slowing down the neutrons: a low value of the spectrum index characterizes an environment capable of thermalizing neutrons), the number of fissions due to ^{235}U, ^{238}U, and ^{239}Pu, the duration of the reaction and its age (Hagemann et al., 1974, 1975; Naudet, 1978; Ruffenach, 1979). However, the validity of these parameters depends on the geochemical stability of the elements which have been used for these calculations. Therefore, the determination of the age of the fission reaction by using this approach depends of the geochemical stability of uranium relative to the fission products, mainly the fissiogenic REEs. For this reason, Ruffenach (1978) and Naudet (1991) have studied in detail a bore-hole (SC36) which cross-cuts reactor 2 which is considered as the most important reactor at Oklo. They demonstrated the good correlation between the amounts of U and Th and the $^{235}U/^{238}U$ ratio with the abundance of various fissiogenic REEs, mainly Nd and Sm. This detailed study has also shown that the budget of Nd versus Th is equilibrated suggesting that there was no uranium migration during the reaction and during the time of ^{236}U radioactive decay (which gives ^{232}Th by α emission). Under such conditions the date of the reaction may be obtained by comparing the global amount of fissiogenic Nd (or radiogenic Th) formed per atom of uranium to the mean fluence received on this uranium. The age obtained is 1950 ± 40 Ma.

The main neutronic parameters of the various reactors are summarized in Table 1. These data clearly show that the reactors differ from one another. The fluences range between 0.22 and 1.3×10^{21} n/cm^2 (reactor 2) reflecting various reaction rates. The number of fission Nf/U which corresponds to the number of fission per present time atoms of uranium in the sample range from 0.43 in reactor 7 to 18.5 in the reactor at Okelobondo. Assuming that the age of all the reactors is constant and equal to 1950 Ma, it is possible to calculate the theoretical value of Nf/U for each reactor and to compare this value to measured values. The difference between the two values, d(Nf/U), reflects the stability of uranium relative to the fission product used for this calculation (Nd in this case). Evidently, the reactors were not perfectly closed systems for uranium and the fissiogenic REEs.

Table 1

Nuclear parameters of the various reactors

Sample	SC36	GL2481	GL.13	SF.84	D.81N	SD.37	OK.84	BA.145
Reactor	2	7	9	10	10	13	Okelo.	Bangombé
FLUENCE	1.45	0.22	0.75	0.56	0.85	0.78	0.33	0.31
C	0.39	0.53	0.80	0.38	0.24	0.11	0.70	0.48
Spectrum ind.	0.17	0.17	0.10	0.16	0.21	0.24	0.14	0.20
(Nf/U)Nd %	3.3	0.43	0.45	1.80	2.20	2.00	18.5	0.75
d(Nd/U) %	4	-28	-80	31	16	17	2100	-7.60
d (x103y)	620	350	320	190	85	22	270	300

Fluence in 10^{21} n/cm^2. C= restitution factor. (Nf/U)Nd = number of fission versus present time uranium content calculated with Nd; d(Nd/U) = difference in % between the theoretical number of fission if fission reaction occurred 1,95 b.y ago and the actual number of fission. d = duration of the fission reactions.

Analytical data are from : reactor 2 : Ruffenach 1979; reactor 7 : Loss et al., 1984; reactor 9 : Curtis et al., 1989; reactor 10, SF84 : Hidaka et al., 1993a; reactor 10, D81N, reactor 13, reactors of Okelobondo and Bangombé : Holliger 1995.

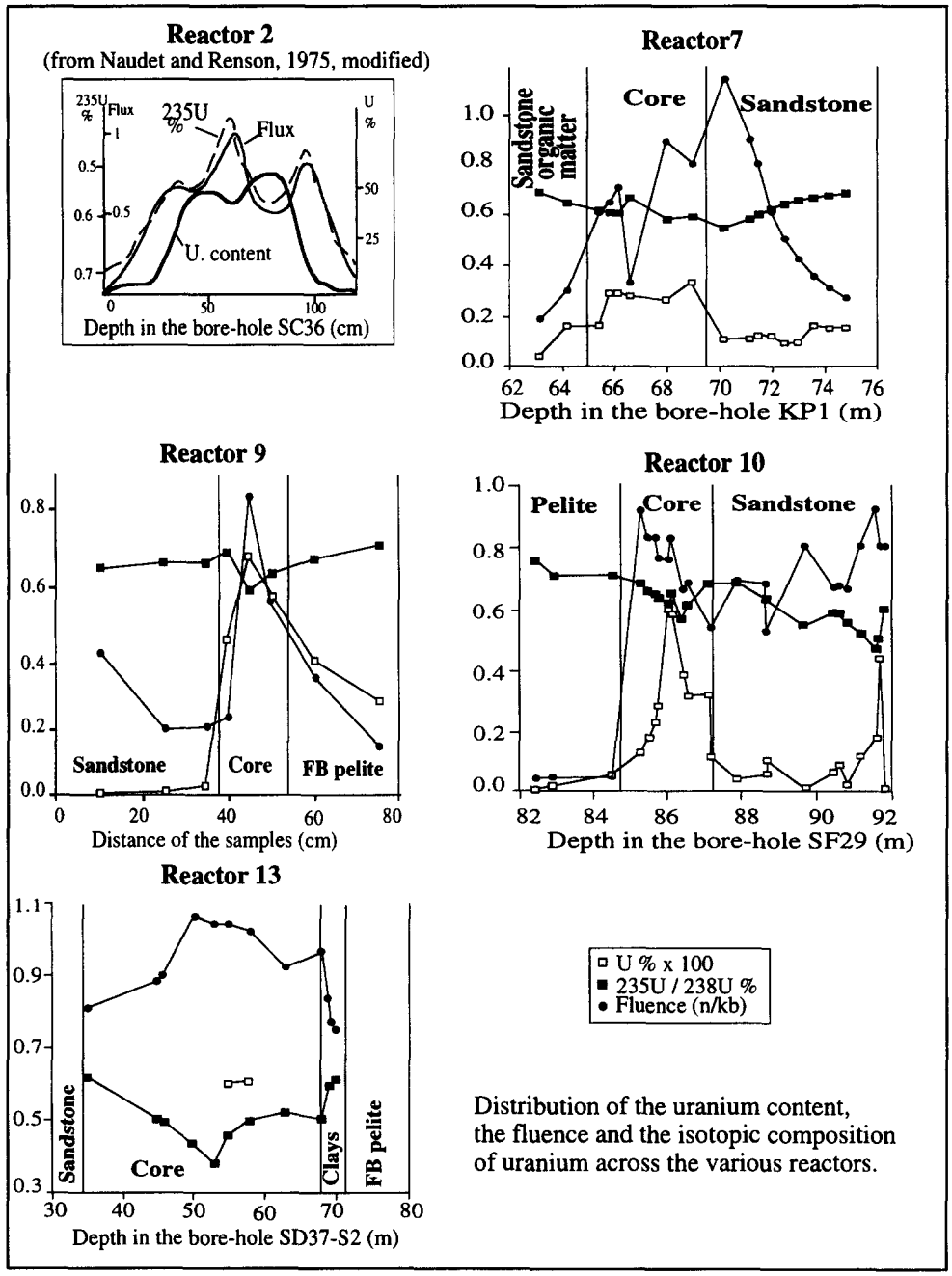

Distribution of the uranium content, the fluence and the isotopic composition of uranium across the various reactors.

FIG. 3. Distribution of the uranium content, the fluence, and the isotopic composition of uranium across the various reactors.

Thus, bore-hole SC36, studied by R. Naudet, appears to represent a specific rather than a general case for natural fission reactors.

The distribution of the reaction rates for the various reactors is illustrated by Fig. 3 and compared to reactor 2, previously analyzed by Naudet (1991). Generally there is good agreement among the uranium content, the $^{235}U/^{238}U$ ratio, and the fluence calculated using the Nd isotopes which have a high neutron capture cross section. It is interesting to note that the higher fluence is located in the sandstones of the reactor 7, at the edge of the core of the reactor where the uranium content is low. This illustrates the effect of the sandstones as reflector of neutrons which has already been discussed for reactor 2 by Naudet (1991). Because the water-uranium ratio in the sandstone is higher than in the clay and the core of the reactor, the sandstone is an environment favorable for the slowing down of the neutrons, whereas the core of the reactor is more absorbent for neutrons. As a consequence, at the interface between these two environments, the thermal neutron flux rises markedly.

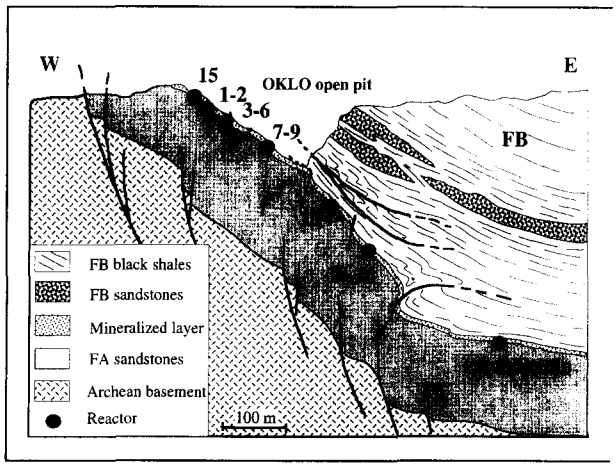

FIG. 4. Cross section of the Oklo and Okelobondo deposits with the projection of the reactors at their different levels.

Four main conditions must be achieved to initiate fission reaction. First, the uranium content should be high in order to reach the critical mass. Second, the geochemical environment should have a low content in poison elements such as B and REEs which are neutron-capturing nuclei. Third, the environment should be rich in light nuclei (hydrogen from water) which act as a neutron moderator and allows for the regulation of the nuclear reaction. And finally, the uranium ore must have high concentration of fissionable nuclei. This last condition is a result of the age of the ore deposit; since the half-life of ^{238}U is about six times the half-life of ^{235}U (4.468×10^9 and 0.7038×10^9 years, respectively), the concentration of ^{235}U in a 2.0 billion years old natural uranium deposit was 3.7% as compared to 0.725% at present. This partly explains why natural reactors have not been found in other high grade uranium ore deposits which are usually younger than Oklo (Dahlkamp, 1993).

The temperatures of the fluids in the reactors and during criticality have been the subject of many different studies based on microthermometric measurements of fluid inclusions (Openshaw et al., 1978; Gauthier-Lafaye, 1986), isotopic compositions of the oxygen in silicates and carbonates (Gauthier-Lafaye et al., 1989) and isotopic composition of Lu, of which the $^{176}Lu/^{175}Lu$ ratio closely depends on the average equilibrium temperature of the neutron at the time of the nuclear reactions (Holliger and Devillers, 1981). Fluid inclusions were studied in quartz overgrowths of the sandstones located at various distances from the reactors, in euhedral quartz, calcites infilling fractures, and apatites. The results show two temperature regimes (Gauthier-Lafaye, 1995): high temperatures for fluid inclusions in quartz located in the surrounding sandstones and fractures (400 to 500°C); and low to medium temperatures for fluid inclusions located in apatites and calcites (100 to 300°C). The high temperatures may represent the temperature of the fluids during criticality, whereas the temperatures of fluid inclusions in apatites range between the temperature of the diagenesis and that of the nuclear reaction. This suggests that the apatites crystallized during the cooling of the reactors. Furthermore, at the edge of the reactor 10, fluid inclusions containing O_2 and H_2 were found (Savary and Pagel, 1993) by Raman spectroscopy and are interpreted as resulting from the radiolysis of the water (Dubessy et al., 1988). Isotopic compositions of oxygen of the clays located in the reactors reveal that during their crystallization a high thermal gradient of 100°C/m occurred between the core and the surrounding rocks (Gauthier-Lafaye et al., 1989; Taieb et al., 1993). On the other hand, clays located inside the core of the reactor crystallized after the neutron bombardment stopped and during the cooling of the reactors. The first isotopic compositions of Lu which were measured in the reactor 2 by Holliger et al. (1978) and Holliger and Devillers (1981) gave surprisingly low temperatures during criticality of 280 ± 50°C. The possible migration of Lu during and after reactor operations and especially the uncertainty on the neutron capture section of ^{175}Lu may, however, underestimate the temperature during criticality.

In the Oklo reactors, different quantities of uranium were involved in the fission reactions. Naudet (1991) has calculated that in reactors 1 to 6, $\sim 7 \times 10^5$ kg of uranium have participated in the nuclear reactions and that 607 kg of ^{235}U are now missing. Taking into account the age of the reactors and the contribution of Pu, we can deduce that this corresponds to $\sim 5 \times 10^3$ kg of ^{235}U having undergone fission, which produced an energy of 16 500 MW yr. From these reactors, reactors 1 and 2 are considered by R. Naudet as the most important one, having the highest reaction rate. For each of these reactors alone, 1800 kg of ^{235}U underwent fission. For comparison, in reactors 7 to 9 and in reactor 10 (Holliger, 1995), only 480 and 650 kg of ^{235}U fissioned producing an energy of 1300 and 2000 MW yr., respectively.

4.3. Geology

The main effect of the fission reactions was to create "a hot spot" in the sandstone reservoirs while the uranium mineralization process was still active (Fig. 4). The thermal event created a circulation of hot fluids around the reactors

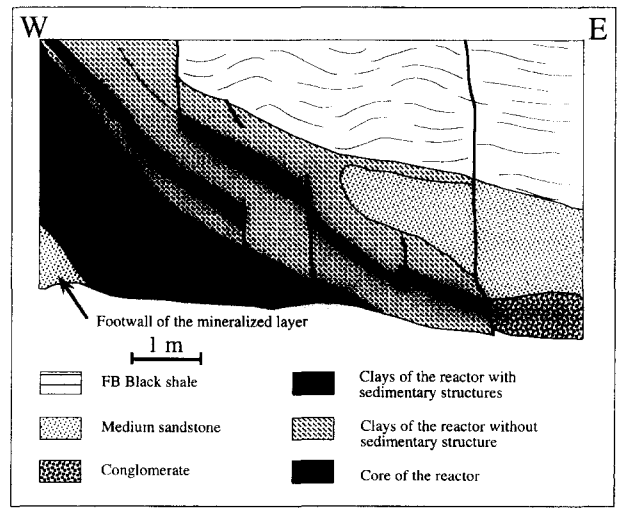

FIG. 5. Cross section in the reactor 2.

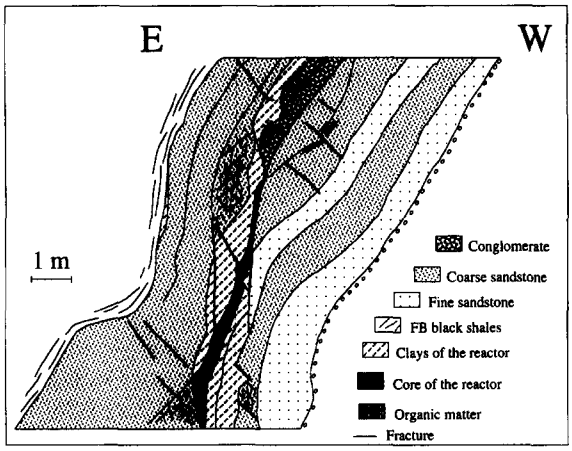

FIG. 6. Cross section of the reactor 9.

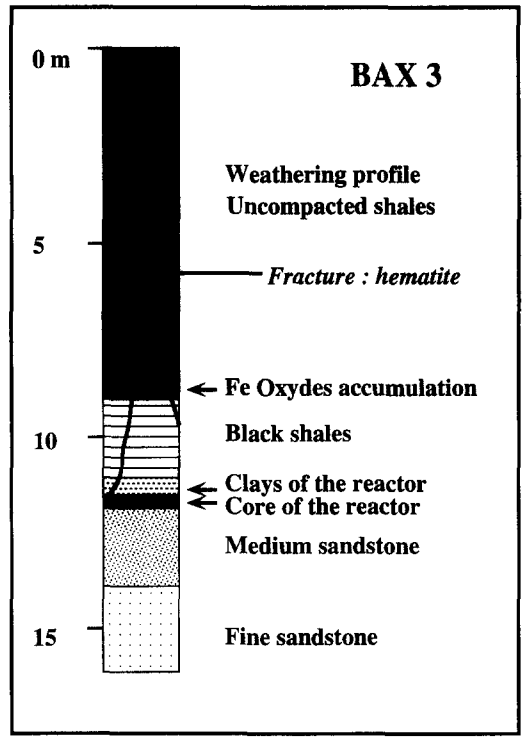

FIG. 8. Stratigraphic Log of the bore-hole BAX 3. Reactor of Bangombé.

and an intense hydrothermal alteration of the host rocks. Modeling of the heat and fluids transfers during criticality have shown that the thermal perturbation around the center of the reactors extends to less than 50 m (Royer et al., 1995). The most apparent effect of this alteration is the disappearance of the sandstones in and around the reactors and their replacement by clays. Eighty percent of the silica migrated out of reactor 2 due to this hydrothermal alteration (Tchibena-Makosso 1982; Gauthier-Lafaye et al., 1989). This alteration also caused a decrease of the volume of the host rocks and their collapse, above and below the reactors.

Typically, all reactors consist of a very high grade uranium ore in which the fission reactions occurred and which is named "reactor core." This facies is surrounded by clays which are named "reactor clays." The uranium content of the core ranges between 20 and 80% whereas in the surrounding clays it decreases to values ranging between a few parts per mil to 1 to 3%. In these two types of rocks several new minerals such as clays, phosphates, oxides, and hydroxides may have crystallized in various proportion depending on local conditions in the reactors.

Reactor 2 has been explored in great detail with more than sixty bore-holes and in six outcrops (Gauthier-Lafaye, 1978). Reactor 2 is a 12 m long and 18 m deep lens; and the thickness of the reactor core ranges between 20 and 50 cm, but which may reach 1 m locally. In this reactor, as well as in reactor 1, all the sandstones of the mineralized layer were affected by the hydrothermal alteration due to the nuclear reaction and were replaced by newly crystallized clay minerals (Fig. 5). Fractures

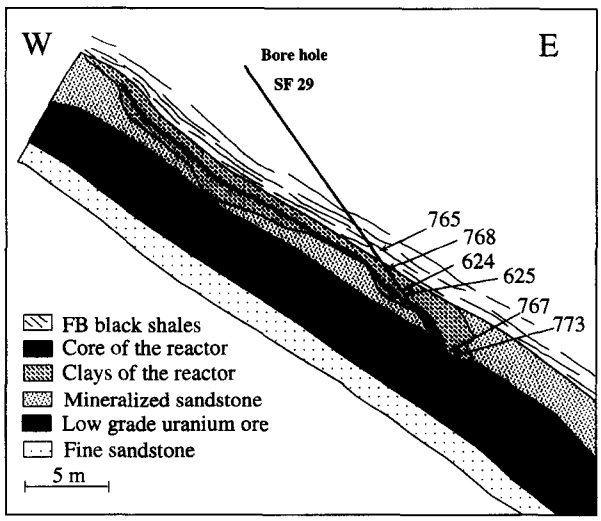

FIG. 7. Cross section of the reactor 10.

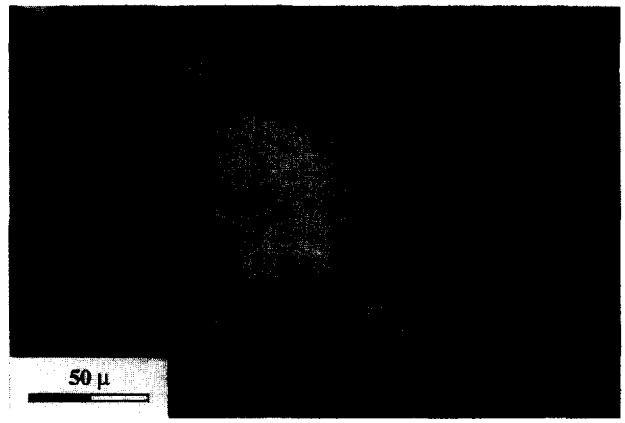

FIG. 9. Crenated uraninite grain from reactor 10 (SF84-1446). Note that indentations seems to follow corridors converging to the center of the grain. Some small grains are isolated from the major grain. Optical microscope, reflected light.

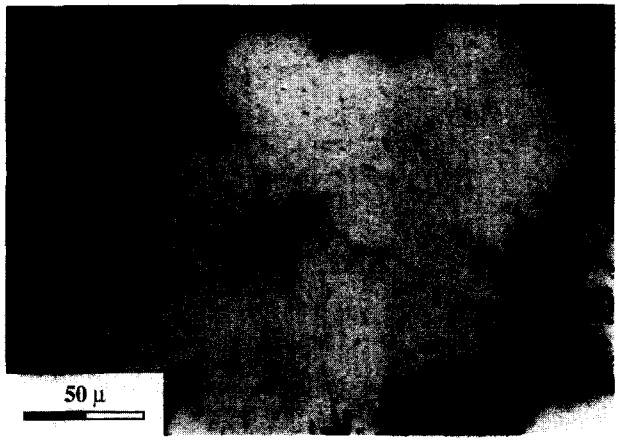

FIG. 10. Crenated uraninite grain with microfractures converging to the center of the grain. Sample from reactor 10 (SF84-1492). Optical microscope, reflected light.

usually form the edges of the reactor suggesting the important role they played as pathways for the hydrothermal fluids. This role is obvious in the reactors 1 and 7 to 9 where sandstones at the bottom of the reactors show intense alteration along fractures, even 10 m from the core of the reactor. Reactors 3 to 6 actually form two reactors named 3–4 and 5–6. They are less important than the previous ones, and sandstones are still preserved around the core. Reactors 7 to 9 are located 200 m deeper than the reactors 1 to 6. In comparison with the previous reactors they appear as small uranium-rich pockets where the core of the reactor is always very thin (a few centimeters), and the hydrothermal clays are never well developed (Fig. 6). In many cases, quartz grains are still preserved in the newly crystallized clays. The characteristic feature of these reactors is the presence of organic matter which may form accumulations of up to few kilograms. This organic matter is particularly abundant at this level of the Oklo deposit, even in mineralized sandstones with no reactors. In the reactors, bitumen is located in the clays of the reactors and even in the core, embedding the uranium oxides which have depleted ^{235}U. Very often, bitumen fills the fractures and is associated with other minerals such as pyrite and galena. Reactor 13 is located 80 m deeper than reactors 7–9 and is located 25 m south of the dolerite dike. We will see in a further section that this location, which is close to the dike, has some importance for describing the behavior of the actinides and fission products. Additionally, this reactor has several other special characteristics. Although reactor 13 is a small reactor (6 m wide and 10 m long), its core has a very high uranium content (up to 87%) with highly depleted ^{235}U ($^{235}U/^{238}U$ = 0.38%). Organic matter does not occur inside the reactor but is abundant in the surrounding sandstones, even in joints affecting the dolerite dike. The clays are almost completely absent in this reactor. Reactor 10 is located 50 m deeper than reactor 13 and 75 m north of the dolerite dike. Among the new reactors, this is the most studied. Reactor 10 has been described from thirteen bore-holes and five wall-faces in drifts. This reactor is up to 30 m wide and 27 m long (Fig. 7). The core as well as the clays are well developed resulting in the collapse of the top of the reactor. As for reactors 7–9, organic matter is abundant in and around the reactor. Apatite crystals millimeters in size were described for the first time in the clays of this reactor, whereas apatite was also found later in reactors 13 and 16. Apatite fills the microfractures affecting the clays and/or are dispersed in the clay matrix. Iron-oxides form a very thin border of millimeter thickness in the sandstones at the boundary with the clays and the core of the reactor. Hydraufracturing is particularly intense in this reactor but also affects reactors 13 and 16. Usually, hydraulic fractures are filled with calcite and minor amounts of sulfides (pyrite), iron oxides, organic matter, and uranium oxides. Reactor 16 is located at the same level as reactor 10 but 80 m north. Reactor 16 was the last reactor to be discovered at Oklo in May, 1991, and is therefore poorly described. However, a wall-face in a drift allowed the preliminary conclusion that it is similar to the reactor 10. The reactor of Okelobondo (also named OK84) is located 60 m below reactors 10 and 16 and 550 m south of the dolerite dike. This reactor has only been recognized in drill-holes and is located on the limb of a narrow syncline and is therefore affected by an intense fracture network. Clays are not well developed, but organic matter has been found in abundance in and around the reactor.

Among all the reactors, the reactor of Bangombé is a very specific type in that it is located only 12 m from the surface and is therefore subjected to weathering (Bros et al., 1994). The reactor has only been recognized in two bore-holes (BA145 and BAX3) and is therefore not well described. In bore-hole BAX 3 (Fig. 8), the core of the reactor is relatively thin (10 to 15 cm) and the hydrothermal clays are mainly developed at the top. Organic matter is abundant in the reactor. The clays are overlain by a 2.5 m thick black-shale layer strongly enriched in organic matter and affected by fractures filled with Fe and Mn oxides. Closer to the surface brown to rubefied pelites occur resulting from supergene weathering of the shales. The interface between black-shales and weathered pelites is marked by strong Fe-oxide accumulations corresponding to a major redox front.

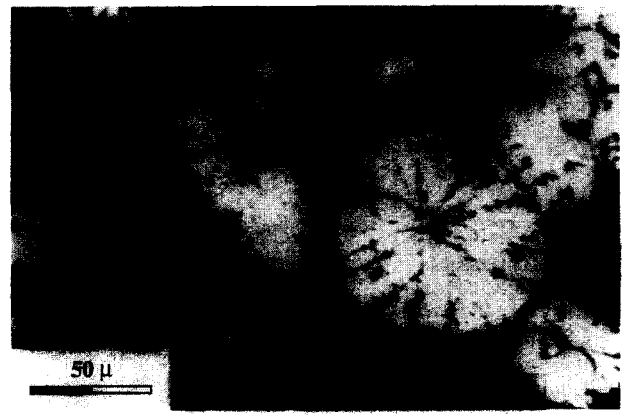

FIG. 11. Uraninite grain with well developed radiating microfractures and small cubic grains. Sample from reactor 10 (SF84-1469). Optical microscope, reflected light.

5. PETROGRAPHY AND GEOCHEMISTRY

5.1. Uranium Oxides

5.1.1. Description of uranium oxides

In the reactors uranium is mainly found as uraninite with some coffinite. In the core of the reactors uraninite forms a massive ore and consists in cubic, cubo-octahedral, and octahedral crystals (Geffroy, 1975; Gauthier-Lafaye, 1986; Janeczek and Ewing, 1995b). In reactor 2, Dran et al. (1978) have described remnants of radiation damages in uraninites due to the fission reaction indicating the stability of these minerals since the criticality. Some typical structures of uraninite are found at Oklo and shown in photos 1–3. Grains show crenellated ("scrappy") edges (Fig. 9 to 11) responsible for the "structure en roue dentée" (cog-wheel structure) described first by Geffroy (1975). When this structure is well developed, edges are "scrappy" and some micrograins (few micron) of uraninite may be isolated from the main grain giving the image of scattered grain in the matrix (Fig. 9). Cracking of the grains is also usual with cracks converging to the center of the grains (Figs. 10 and 11). Most often, these features do not show special evidence for alteration such as coffinitization or development of secondary phases,

Table 2

Electron microprobe analyses of uranium oxides from reactors 7, 8, 10, 13.

Samples	UO2	PbO	CaO	SiO2	TiO2	FeO	K2O	Pb/UO2
Out of the reactors								
Ur-1 (5)	87.55	4.83	1.02	2.40	0.15	0.27	-	0.055
Reactor 2								
733 (24)*	89.10	6.02	1.58	0.80	<0.1	0.42	-	0.067
Reactor 7								
Ur-1 (5)	87.56	4.45	1.30	0.84	1.16	0.50	0.13	0.051
Reactor 8								
Ur-1 (5)	89.08	4.79	0.93	0.51	0.05	0.28	0.14	0.054
Reactor 9								
9-005 (19)*	88.76	5.87	1.67	0.72	0.18	0.54	-	0.066
Reactor 10. Bore hole SF42. 27m40								
Ur-1 (30)	77.89	15.36	1.92	1.20	0.02	0.05	0.12	0.197
Ur-2 (19)	78.57	14.32	1.59	1.16	0.05	0.05	0.12	0.182
Ur-3 (39)	78.80	14.57	1.69	1.17	0.02	0.04	0.11	0.185
Ur-4 (38)	77.06	18.05	1.16	0.89	0.02	0.02	0.12	0.234
Reactor 10. Bore hole SF29. 86m42								
Ur-1 (5)	85.40	6.47	1.82	1.43	0.10	0.60	0.05	0.076
Reactor 10. Bore hole SF29.90m85								
Ur-1 (5)	84.40	5.63	1.01	3.28	0.35	0.60	0.15	0.067
Reactor 10. Bore hole SF29.91m67								
Ur-1 (49)	79.50	12.87	1.28	0.70	0.34	0.32	0.12	0.162
Ur-2 (15)	79.56	12.28	1.48	0.79	0.43	0.35	0.11	0.154
Reactor 10. Bore hole SF84.14m85								
Ur-1 (5)	80.64	11.75	1.32	0.83	0.20	0.25	0.05	0.146
Reactor 10. Bore hole SF85.19m20								
Ur-1 (5)	83.52	7.39	1.30	1.90	0.92	0.48	0.14	0.088
Coff-2 (5)	75.48	0.47	1.58	15.46	0.05	0.05	0.13	0.006
Reactor 13. Bore hole SD37-S2-CD								
Ur-1 (21)	86.14	5.57	1.92	0.52	<0.02	0.30	0.12	0.065
Ur-2 (26)	86.91	5.49	1.94	0.53	<0.02	0.25	0.15	0.063
Ur-3 (50)	87.00	5.48	1.95	0.55	<0.02	0.35	0.12	0.063
Ur-4 (10)	87.84	6.10	1.54	0.54	<0.02	0.26	0.13	0.069
Ur-5 (11)	86.63	5.54	1.80	0.52	<0.02	0.40	<0.05	0.064
Reactor 16								
D75-1 (14)*	90.54	5.63	1.19	0.30	0.14	0.50	-	0.062

Data are given in weight %. ( ) : Number of analyses; * = data from Janeczek and Ewing 1995.

FIG. 12. Coffinite (C) replacing a chlorite mineral in the core of the reactor of Bangombé. P = pyrite, g = galena. Optical microscope, reflected light.

thus suggesting that they developed during or soon after the precipitation of the uraninite grains. When coffinitization occurs, it usually starts at the edges of the grains or at its center when it is pierced throughout (Janeczek and Ewing, 1992, 1995b).

Coffinitization of uraninite grains, starting usually at the edges of the grains, may be more or less well developed (Eberly et al., 1994). In the most weathered reactor of Bangombé, coffinite may represents a major phase in the core of the reactor and in some cases it replaces newly crystallized chlorites (which crystallized during the fission reactions: see further section), suggesting an important remobilization of uranium after the reactor operation (Fig. 12). Galena is mainly made of radiogenic lead and is a common phase occurring as inclusions in the uraninite grains and in the matrix of the core of the reactors.

5.1.2. Major elements and uranium-lead isotopic analyses

Uranium oxides were analyzed for major element contents and uranium and lead isotopic compositions (Holliger, 1995, Janeczek and Ewing, 1995b). Table 2 shows the chemical composition of uraninites from the different reactors. Beside the lead contents which vary from one reactor to another, the chemical compositions of uraninites are very similar whatever the reactor, suggesting similar geochemical conditions of precipitation of uranium oxides in the various reactors. On the other hand, the Pb/U ratios are scattered suggesting an important lead mobilization (Janeczek and Ewing, 1995b).

The isotopic compositions of lead obtained by SIMS analyses on galena from the various reactors and of samples located outside the area of influence of the reactors (100 m

Table 3
Lead isotopic compositions, apparent ages of galena and age of lost of lead.

Reactor #	Sample	235/238 U %at.	204/206 Pb	207/206 Pb	208/206 Pb	207/206(a) Pb/Pb	207/206(b) Pb/Pb	Age(b) Ma	AgeT2 Ma
	Galena								
2	SC48bis-2283	0.680	0.001348	0.15480	0.07590	0.13708	0.14635	2200	690
3	SC55-1853	0.680	0.000218	0.13778	0.01022	0.13491	0.14426	2280	640
8	F229D.GL2885	0.654	0.000276	0.14543	0.01308	0.14182	0.15743	2430	910
8	F229D.GL2903	0.672	0.001610	0.15850	0.06260	0.13730	0.14830	2320	730
8	F299C.11a	0.710	0.000257	0.14243	0.01261	0.13906	0.14220	2250	600
8	F299C.11b	0.710	0.000265	0.14542	0.01297	0.14196	0.14516	2290	660
8	GL11.2983	0.680	0.000234	0.14034	0.01168	0.13726	0.14654	2300	690
8	GL11-2991.C1f	0.720	0.000361	0.15490	0.01973	0.15023	0.15148	2360	790
8	KP13	0.680	0.000264	0,14470	0.01281	0.14125	0.15080	2350	780
10	SF29-8612/1	0.630	0.000253	0.15249	0.01240	0.14922	0.17275	2580	1180
10	SF29-8612/2	0.630	0.000264	0.14603	0.01138	0.14259	0.16480	2500	1040
10	SF29-8642/1	0.579	0.000190	0.12440	0.00914	0.12186	0.15340	2380	830
10	SF29-9066/1	0.560	0.000014	0.10431	0.00668	0.10412	0.13497	2160	420
10	SF29-9167/1	0.520	0.000143	0.12810	0.00919	0.12620	0.17618	2620	1230
10	SF85-1920	0.685	0.000320	0.14570	0.01151	0.14150	0.15000	2350	760
10	D81N-040292/II	0.700	0.000270	0.14520	0.01255	0.14170	0.14690	2310	695
10	D81N190292/4	0.650	0.000240	0.14070	0.01103	0.13760	0.15360	2380	830
13	SD37-26	0.710	0.000700	0.15555	0.04350	0.14650	0.14980	2345	760
13	37S2108	0.580	0.000120	0.11743	0.00984	0.11610	0.14562	2290	670
13	37S2109	0.600	0.000200	0.12565	0.02149	0.12300	0.14934	2340	750
13	37S2CD8	0.465	0.000312	0.12990	0.01382	0.12575	0.19630	2800	1530
13	37S2/46 cm	0.490	0.000340	0.14000	0.01418	0.13550	0.20000	2820	1550
13	37S2/58 cm	0.510	0.000258	0.13160	0.01110	0.12820	0.18250	2670	1350
13	37S2/70 cm	0.580	0.000190	0.11120	0.00883	0.10860	0.13590	2170	450
16	D75-11.91/23-2	0.660	0.000360	0.14290	0.01690	0.13820	0.15200	2370	800
16	D75/1	0.632	0.000340	0.13640	0.01596	0.13190	0.15150	2360	790
	Pb métal								
10	SF29-8525/1	0.684	0.000120	0.10160	0.00614	0.09997	0.10602	1725	-
10	SF29-8525/2	0.684	0.000130	0.10170	0.00613	0.09992	0.10597	1724	-
	Metallic agregat								
13	37S2CD2	0.382	< 0.0005	0.12660	0.01413	0.12158	0.23106	3060	1900
13	37S2CD5	0.382	< 0.0005	0.12590	0.01376	0.11489	0.23928	3115	1900
Out of the reactors									
	Okelo.OD11-132	0.710	0.002546	0.17800	0.12630	0.14490	0.14817	2320	725
	ES24-13	0.726	0.000497	0.14912	0.02092	0.14264	0.14264	2260	610
	RO33-23	0.726	0.000387	0.13144	0.01638	0.12630	0.12630	2050	200
	OKLO								
	PUITS46m	0.726	0.041560	0.69900	2.10340	-	-	-	
	C2-290m	0.726	0.059410	0.91873	2.17270	-	-	-	-
	C2 (20m ss C1)	0.726	0.010722	0.29347	0.58719	0.15550	0.15550	2410	870
	C1 (Oklo Nord)	0.726	0.005821	0.22939	0.32830	0.15440	0.15440	2400	850
	OTOBO-KA13	0.726	0.053700	0.84950	2.41400	-	-		

(a): isotopic composition of radiogenic lead. Correction for common lead: 206/204=15.2. 207/204=15.2.
(b): isotopic composition of radiogenic lead and apparent age after correction for ^{235}U depletion.
T2: age of lost of lead for an primary uranium mineralization age of 1.95 Ma.
Data were determined by secondary ion microscope mass spectrometer (SIMS) using the CAMECA IMS3F on individual uranite (for $^{235}U/^{238}U$) and galena crystals. Typical spot analyzed was 20 μm in diameter. 2σ error range is 0.1% and 0.3% for Pb isotopic ratios and $^{235}U/^{238}U$, respectively. Detailed method is described in Cathelinau et al. (1990).

to 3 km from the reactors) are reported in Table 3. Apparent Pb-Pb ages range from 2050 Ma to 2580 Ma and the age of loss of lead from the uraninites (T2), assuming that the age of uranium precipitation is 1950 Ma (Ruffenach, 1979; Naudet, 1991), ranges from 450 to 1550 Ma. The distribution of the ages on an histogram (Fig. 15) shows a maximum of data between 700 and 800 Ma which is close to the age of intrusion of the dolerite dike (Bonhomme et al., 1982).

U-Pb ages were determined on various uraninite grains of samples from the reactors 9, 10, 13, and on a sample located 50 m away from the reactors (ES24) (Table 4). In reactor 10, samples from bore-holes SF29 and SF42 were analyzed. In bore-hole SF42 (sample 2740), U-Pb analyses were performed on two single euhedral grains of uraninites enclosed in organic matter and showing a zonation of alternating Ca and Pb rich layers (Fig. 13). In bore-hole SF29, the analyzed uraninite grains are located in sandstones which are in contact with the core of the reactor. On a classic U-Pb concordia diagram (Fig. 16), data points for these two bore holes fit on two discordia yielding ages of 1968 ± 50 (SF42) and 2018 ± 30 Ma (SF29). These ages are in good agreement with those obtained from the U-fission product pairs of uraninites of the reactors and the U-Pb data on bulk rocks ores of Oklo (Devillers et al., 1975; Lancelot et al., 1975; Gancarz, 1978). This result confirms that reactor 10 has not been affected by any im-

Table 4
SIMS analyses. Isotopic compositions of U and Pb of uraninites and Pb/U ratios.

Spot n°	U 235/238	Pb 204/206	Pb 207/206	Pb 208/206	Pb rad 207/206	U/Pb 207/235	U/Pb 206/238
Reactor 9. Sample GL3535							
1	0.00650	0.000046	0.0689	0.00211	0.0763	1.065	0.1013
2	0.00690	0.000029	0.0620	0.00112	0.0648	0.825	0.0924
3	0.00688	<0.00004	0.0634	0.00121	0.0664	0.904	0.0988
4	0.00645	<0.00004	0.0618	0.00131	0.0691	0.860	0.0903
5	0.00690	0.000032	0.0625	0.00124	0.0653	0.848	0.0943
6	0.00663	0.000056	0.0717	0.00253	0.0778	0.973	0.0909
7	0.00665	0.000063	0.0698	0.00252	0.0753	0.900	0.0867
8	0.00702	0.000031	0.0636	0.00137	0.0653	0.793	0.0882
Reactor 10. Bore hole SF42							
U1/1	0.00710	0.000035	0.1109	0.00138	0.1129	3.550	0.2280
U1/2	0.00708	0.000023	0.1201	0.00086	0.1228	4.610	0.2720
U1/3	0.00692	0.000031	0.1092	0.00126	0.1141	2.580	0.1640
U1/4	0.00706	0.000025	0.1180	0.00108	0.1210	3.400	0.2040
U1/5	0.00710	0.000020	0.1196	0.00072	0.1221	4.340	0.2580
U1/6	0.00666	0.000035	0.1079	0.00155	0.1170	3.140	0.1950
U1/7	0.00710	0.000032	0.1129	0.00126	0.1150	2.210	0.1390
U2/8	0.00685	0.000022	0.1143	0.00093	0.1208	4.900	0.2940
U2/9	0.00688	0.000025	0.1122	0.00105	0.1180	4.170	0.2560
U2/10	0.00690	0.000028	0.1122	0.00125	0.1176	4.380	0.2700
U2/11	0.00690	0.000024	0.1132	0.00096	0.1188	4.990	0.3040
Reactor 10. Bore hole SF29. SANDSTONE							
88.70/1	0.00663	0.000070	0.08016	0.00270	0.07918	0.859	0.0787
89.70/1	0.00575	0.000058	0.08019	0.00294	0.10014	1.621	0.1173
90.66/1	0.00612	0.000065	0.10924	0.00261	0.10829	1.753	0.1174
90.85/1	0.00569	0.000090	0.09271	0.00360	0.09148	1.422	0.1127
91.20/1	0.00521	0.000100	0.11425	0.00444	0.11290	1.435	0.0922
91.66/1	0.00515	0.000075	0.11974	0.00309	0.11874	3.942	0.2408
91.67/1	0.00482	0.000087	0.12434	0.00349	0.12318	4.641	0.2733
91.67/2	0.00427	0.000057	0.12622	0.00332	0.12546	3.075	0.1778
91.67/3	0.00518	0.000090	0.12510	0.00362	0.12390	3.536	0.2070
91.67/4	0.00485	0.000067	0.12043	0.00338	0.11953	2.334	0.1417
91.68/1	0.00549	0.000070	0.11711	0.00291	0.11618	2.853	0.1782
REACTOR 13. DRIFT SD37.							
35	0.00616	<0.00003	0.0593	0.00162	0.0694	0.819	0.0857
45	0.00495	<0.00003	0.0451	0.00233	0.0656	0.745	0.0823
46	0.00490	<0.00003	0.0455	0.00218	0.0668	0.676	0.0734
50	0.00430	<0.00003	0.0410	0.00290	0.0685	0.793	0.0836
55	0.00446	<0.00003	0.0401	0.00260	0.0646	0.595	0.0666
58	0.00490	<0.00003	0.0462	0.00255	0.0679	0.676	0.0720
68	0.00498	<0.00003	0.0459	0.00246	0.0663	0.735	0.0802
69	0.00585	<0.00003	0.0529	0.00204	0.0652	0.764	0.0850
70	0.00600	<0.00003	0.0810	0.00536	0.0976	0.759	0.0661
Out of the reactor. Drift ES24.							
4-1	0.00726	0.000024	0.0636	0.00084	0.0633	0.665	0.0763
4-2	0.00726	0.000021	0.0631	0.00076	0.0628	0.576	0.0665
4-3	0.00726	0.000012	0.0618	0.00048	0.0616	0.612	0.0720
4-4	0.00726	0.000019	0.0621	0.00064	0.0619	0.437	0.0512
4-5	0.00726	0.000024	0.0638	0.00093	0.0635	0.713	0.0814
4-6	0.00726	0.000025	0.0638	0.00091	0.0634	0.547	0.0626
4-7	0.00726	0.000015	0.0627	0.00078	0.0625	0.624	0.0724
4-8	0.00726	0.000015	0.0623	0.00059	0.0620	0.662	0.0774
13-1	0.00726	0.000015	0.0630	0.00068	0.0627	0.887	0.1026
13-2	0.00726	0.000020	0.0627	0.00059	0.0623	0.860	0.1002
13-3	0.00726	0.000018	0.0635	0.00066	0.0632	0.876	0.1006
13-4	0.00726	0.000014	0.0644	0.00058	0.0641	0.964	0.1091
13-5	0.00726	0.000025	0.0645	0.00099	0.0641	0.906	0.1026

(a) : Ratio corrected for 235U/238U.

portant alteration event which would have caused dissolution and recrystallization of uranium oxides.

In reactor 13, the center of the uraninite grains is devoid of galena inclusions (very low Pb/U ratio, Table 4) which are in turn concentrated at the edges of the grains (Fig. 14) and in the matrix, against the uraninite grains. U-Pb isotopic analyses were made in the center of the uraninite grains and give an age of 850 ± 50 Ma on the concordia diagram (Fig. 17). This age also corresponds to the major loss of lead as seen before and is related to the extensional event affecting the basin at the time of intrusion of the dolerite dike. Uraninite grains of sample ES24 located 50 m further from the dolerite dike also show an episodic loss of lead at the same time (722 ± 30 Ma) as shown on the concordia-discordia diagram (Fig. 17). For reactor 9, data points are scattered

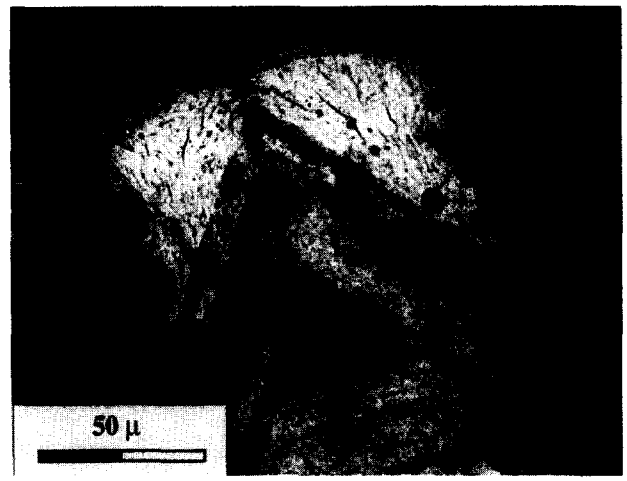

FIG. 13. Zoned uraninite from reactor 10 (SF42). White and dark areas are Pb and Ca-rich zones. SEM photomicrograph.

on $^{206}Pb/^{238}U$-$^{207}Pb/^{235}U$ diagram suggesting a complex history for both lead and uranium.

5.1.3. *Fission products*

Previous work on reactor 2 (Naudet 1991; Ruffenach 1979) and 7 to 9 (Loss et al., 1988, 1989; Hidaka et al., 1988) as well as new data obtained on reactors 7 to 13 (Hidaka et al., 1992) allow one to determine the behavior of the fission products in uraninite grains and to consider two types of elements depending on their degree of retention within these grains. Most of the data presented here come from analyses made on bulk rocks of uranium rich samples from the core of the reactors.

Elements which are considered stable elements in the uraninite are mainly the actinides, transuranium elements (Np, Pu, Am and Cm), platinum metals (Ru, Rh, Pd), Te, Y, Nb, Tc, Bi, Th, REEs, and Zr. All of these elements have a ionic radii similar or close to that of uranium favoring their

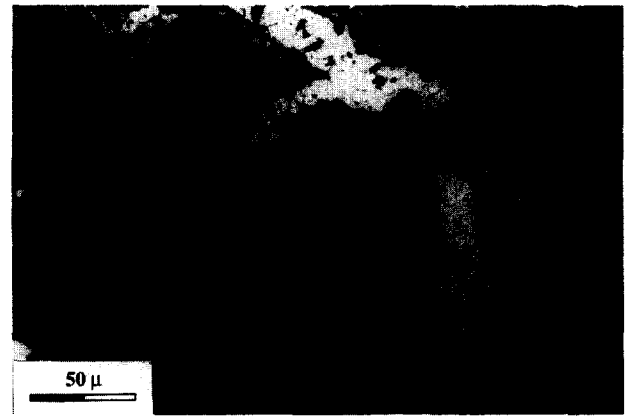

FIG. 14. Uraninite grain from reactor 13 (SD37-S2). Note that the center of the grain is devoid of galena inclusions (white) which are concentrated at its edges. Optical microscope, reflected light.

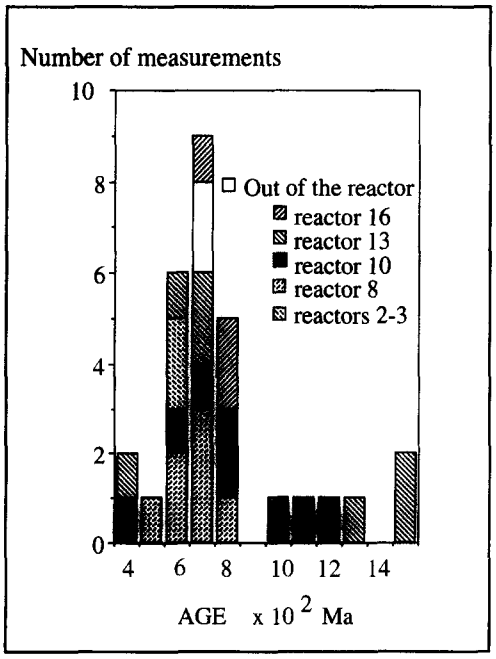

FIG. 15. Histogram of Pb-Pb ages of galenas. The age T2 of the galena is obtained assuming primary uranium mineralization age of 1950 Ma.

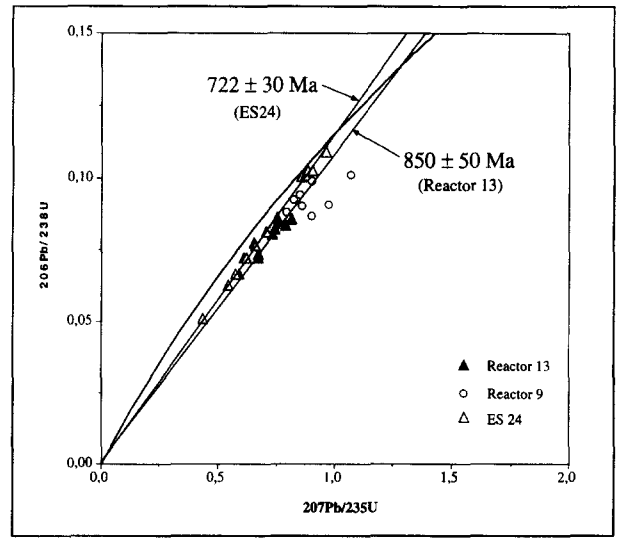

FIG. 17. Concordia plot showing U/Pb isotope analyses by SIMS of uraninite grains from reactors 9 and 13 and from an uranium ore out of the reactors (ES24).

retention in the uraninite structure. Studying in more detail the behavior of these elements, it appears however that Ru was more mobile than the other platinum metals. It has been shown that a small proportion of fissiogenic Ru may be found in the clays matrix of the core of the reactor and in the clay surrounding the core as well as in sandstones located 12 m from the reactors (Gancarz et al., 1980; Loss et al., 1989; Naudet, 1991). Similarly, Tc which has no stable isotope in nature, and the isotope of which ^{99}Tc is the precursor of ^{99}Ru has also partially migrated during the fission reactions (Hidaka et al., 1993b). Recently, Hidaka et al. (1995) have evidenced an excess of ^{90}Zr in the core of reactor 10 which is due to migration of its precursor ^{90}Sr ($t_{1/2}$ = 29.1 y) during criticality. We will discuss in a later section that partial proportion of platinum metal, Te and Bi (Bi is the stable radiogenic daughter of ^{237}Np, $t_{1/2}$ = 2.14 Ma) may also have moved out from the uraninite grains in reactor 13.

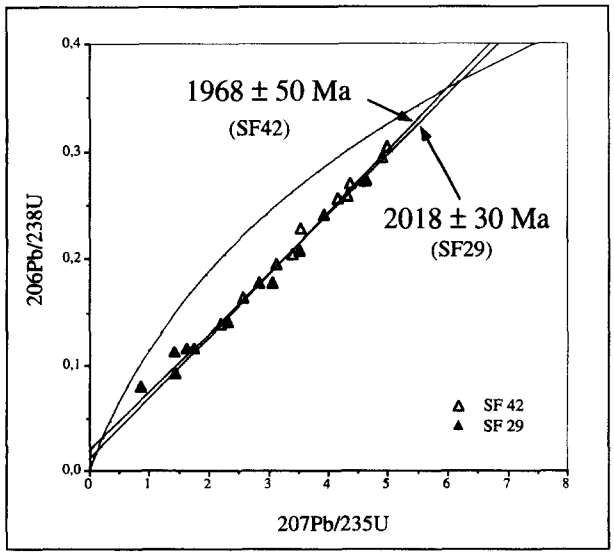

FIG. 16. Concordia plot showing U/Pb isotope analyses by SIMS of uraninite grains from reactor 10.

Fission products which were not retained in the uraninite structure are mainly noble gases (Xe, Kr), halogen (I), Cd (a volatile element like Cs) (De Laeter and Rosman, 1975; Curtis et al., 1989), Br, alkaline elements (Rb, Cs), earth-alkaline elements (Sr, Ba), Te, Pb, Mo, Sn, and Ag.

Xenon and krypton which are volatile elements with a larger ionic radius than uranium (2.0 and 1.8 for Xe and Kr, respectively, versus 1.04 for U^{4+}) were not stable in such structure. Iodine, of which fissiogenic ^{129}I converts to ^{129}Xe ($t_{1/2}$ = 1,6*10^7 y) have the same distribution as Xe suggesting that both elements have the same behavior (Hagemann and Roth, 1978; Ruffenach, 1979). All these elements have a relatively high fission yield resulting in an important amount of gas produced during and after the fission reaction. It is possible that the migration of these gas out from the uraninite grains is responsible for their special structures: crenellated edges, channels and cracks (Figs. 9 to 11).

Cd was analyzed in reactor 9 (Loss et al., 1989; Curtis et al., 1989) and only traces have been found in the core as well as in the surrounding rocks revealing that Cd has been almost totally removed from its site of production. In all the reactors, Rb, Sr, Ba, and Cs were also almost totally removed. Hidaka et al. (1994a) have estimated that around only 5% of these elements were retained in the core of the reactor 10. In this reactor it has also been demonstrated, by

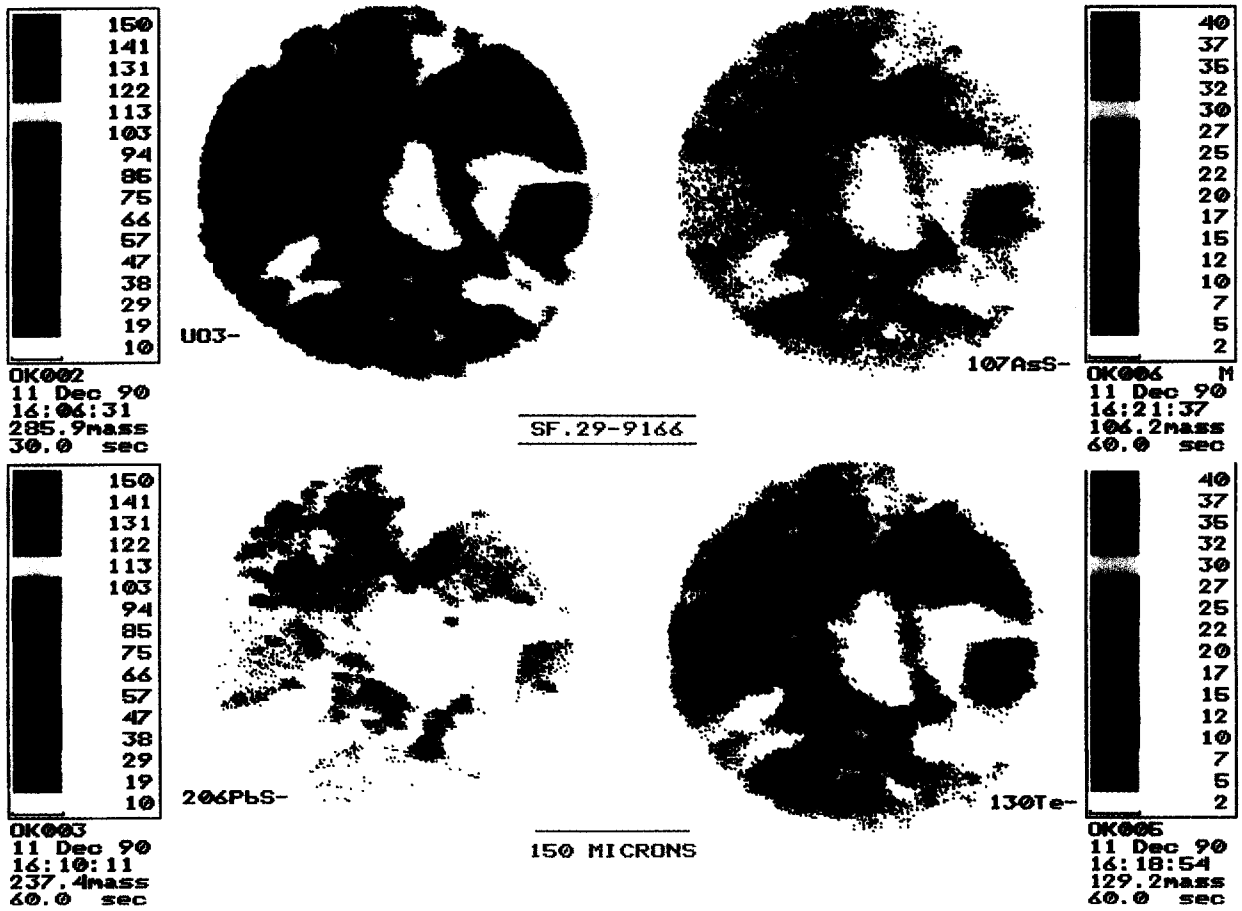

FIG. 18. Distributions of the ionic species ^{107}AsS, ^{206}PbS and ^{130}Te relative to uranium in negative secondary ion mode. SIMS analyses. Sample SF 29-9166. Reactor 10.

analyzing isotopic compositions of Ba, that a fractionation between fissiogenic Cs (^{135}Cs and ^{137}Cs are precursors of ^{135}Ba and ^{137}Ba, respectively) and Ba occurred early during the fission reactions (Hidaka et al., 1993a). Most of fissiogenic Mo and Ag were not retained in uraninite. It has been estimated that only 10% of the fissiogenic Mo remains in reactor 2 (Naudet, 1991), whereas 20% of the fissiogenic Ag may be still present in reactor 9 (Curtis et al., 1989). However, these two elements were substantially found in the vicinity of the reactor 9 (Loss et al., 1989; Janeczek and Ewing, 1995b).

All these results concerning the stability of fission products were confirmed in reactors 10 and 13 by SIMS analyses on uraninite grains (Holliger, 1995). As an example, the distribution of As, Pb, and Te in a uraninite grain is given on Fig. 18 showing the good correlation between uranium and these elements. However, and as discussed before in the context of the nuclear parameters, migration of fission products and actinides have occurred. Table 5 gives the isotopic composition of uranium, Nd/U, and Sm/U ratio measured by SIMS, and the calculated parameters such as the number of fissions relative to the present time uranium content and the age of the fission reaction. For reactor 10, the ages are not constant and range between 0.5 to 2.3 b.y suggesting a geochemical fractionation of the U-Nd-Sm system in the core of the reactor. On the other hand, analyses made on the uraninite grains from reactor 13 are less scattered around a mean value of 2.0 b.y. This constant value is obtained despite the fact that for the same samples, U-Pb and Pb-Pb analyses show high loss of lead during the dolerite intrusion.

5.2. Metallic Aggregates

Metallic aggregates a few microns in size were found for the first time at the edge of the core of reactor 10 (borehole SF29), where uraninite is enclosed in new crystallized quartz. A typical aggregate from this reactor is shown on Fig. 19. The center of the metallic aggregate consists of areas made of Pb-Ru-As-S and Pb-Te phases. The outer part of the aggregate is mainly made of silicate of U and Zr containing microinclusions of Pb-(Se, S) and Pb-Pd. Galena appears as a secondary phase. Later, metallic aggregates were also found in great quantity in the core of reactor 13. In this case, most of the aggregates are located between the uraninite grains and form large patches of 100 μ size (Figs.

Table 5

Isotopic ratios of 235U/238U, 232Th/238U, (143+144)Nd/238U, 147Sm/238U measured in-situ with SIMS on uranium oxides and nuclear parameters calculated from in-situ analyses and from thermoionisation mass spectrometry analyses on bulk-rocks.

Sample	U 235/238	U % w	Th/U % at	Nd/U ppm atom.	Sm/U ppm Atom.	Nf/U (%) Nd	Nf/U (%) Sm	Age 10^9 y. Nd	Age 10^9 y. Sm
Reactor 2									
KN50-3548	*0.4650*	*55.2*				*3.25*	*3.46*	*2.05*	*2.11*
Reactor 7									
KP1-2898	0.6680		0.348	1500	230	1.33	1.07	1.58	1.37
KP1-2898	*0.6680*	*2.1*				*1.50*	*1.60*	*2.04*	*2.10*
Reactor 8									
GL3046	0.5900		0.429	1600	200	1.42	0.93	1.69	1.26
GL3046	*0.5980*	*28.0*				*1.19*	*1.31*	*1.95*	*2.05*
KP1-GL2481	*0.6780*	*41.0*				*0.51*	*0.54*	*1.82*	*1.86*
GL3097	0.6720		0.158	780	115	0.69	0.54	0.95	0.69
Reactor 9									
KP3-4,65m	0.7240		0.013	70	20				
GL3541	0.7250		0.005	<50	<15				
Reactor 10									
SF29-67/1	0.482		0.792	2700	450	2.40	2.10	2.07	2.00
SF29-68/1	0.549		0.503	2840	450	2.52	2.10	2.10	1.97
D73-41	0.6410		0.120	620	100	0.55	0.47	1.29	1.12
D73-88	0.6820		0.214	1740	260	1.54	1.21	1.83	1.92
SF42-2740	0.6950		0.011	400	63	0.35	0.20	0.30	0.61
SF42-2790	0.6600		0.057	1400	240	1.24	1.12	1.67	2.07
SF84-1485	0.5650		0.400	2630	400	2.33	1.87	2.49	2.04
SF84-1485	*0.5649*	*14.9*				*1.97*	*1.85*	*2.25*	*2.18*
SF84-1521	0.6100		0.290	2390	340	2.12	1.59	2.29	1.90
SF84-1469	*0.6048*	*17.2*				*1.63*	*1.64*	*2.19*	*2.20*
SF84-1480	*0.5069*	*7.1*				*1.59*	*1.38*	*1.83*	*1.68*
SF84-1492	*0.5797*	*24.3*				*1.85*	*1.90*	*2.27*	*2.29*
D81N-4II	0.6470		0.370	1560	230	1.38	1.07	1.78	1.52
D81N-12II	0.6580		0.314	1450	230	1.29	1.07	1.69	1.75
D81N-2II	0.6700			890	130	0.79	0.61	1.17	1.23
Reactor 13									
SD37-S2/50	0.4300			3325	645	2.95	3.00	2.2	2.2
SD37-S2/53	0.3750			2685	525	2.38	2.44	2.1	2.1
SD37-S2/CD	*0.4630*	*59.4*				*1.55*	*2.64*	*1.86*	*2.40*
Reactor16									
11.91/23	0.6600		0.156	620	105	0.55	0.49	1.17	1.40
Reactor of Okelobondo									
OK84-2724	*0.6820*	*0.4*				*20.00*	*16.70*	*5.15*	*4.96*
Reactor of Bangombé									
BA145-1160	*0.6552*	*45.0*				*0.83*	*0.92*	*2.01*	*2.10*

Data in italic type are from bulk-rocks samples. Data in normal type are in-situ analyses.

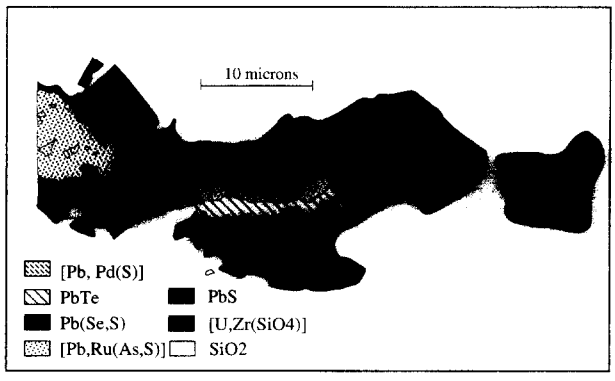

FIG. 19. Metallic aggregate. Distribution of Pb, Te, Se, Ru, As, U, Zr, Si and S. Sample SF29-9166 Reactor 10.

20 and 21). Chemical analyses of the aggregate are reported in Table 6. From these data we must add that Mo and Bi were found together in reactor 13 whereas they were not detected in reactor 10 (Fig. 20). On a diagram plotting the Ru-Rh-Te-As-S contents versus the Pb-S contents (not shown) all data points fit well on a line suggesting that these elements correspond to a mixture of microcrystals of galena and metallic aggregates. Isotopic analyses of Ru (Holliger, 1992; Hidaka et al., 1994b) have shown a heterogeneous distribution of ^{99}Ru (with variations of the $^{99}Ru/^{101}Ru$ ratio) suggesting that these aggregates formed before complete decay of ^{99}Tc to ^{99}Ru ($t_{1/2}$ = : 2.1 10^5 y). The high content of fissiogenic platinum metal elements in the metallic aggregates suggest that they are similar to the insoluble nodules in the spent fuel (Kleykamp, 1985).

Native lead has been found in large amounts in the core and in the surrounding clays of reactor 10, and to a minor extend in reactor 13. The metallic lead is mainly located in microfractures of millimeter size and around uraninite

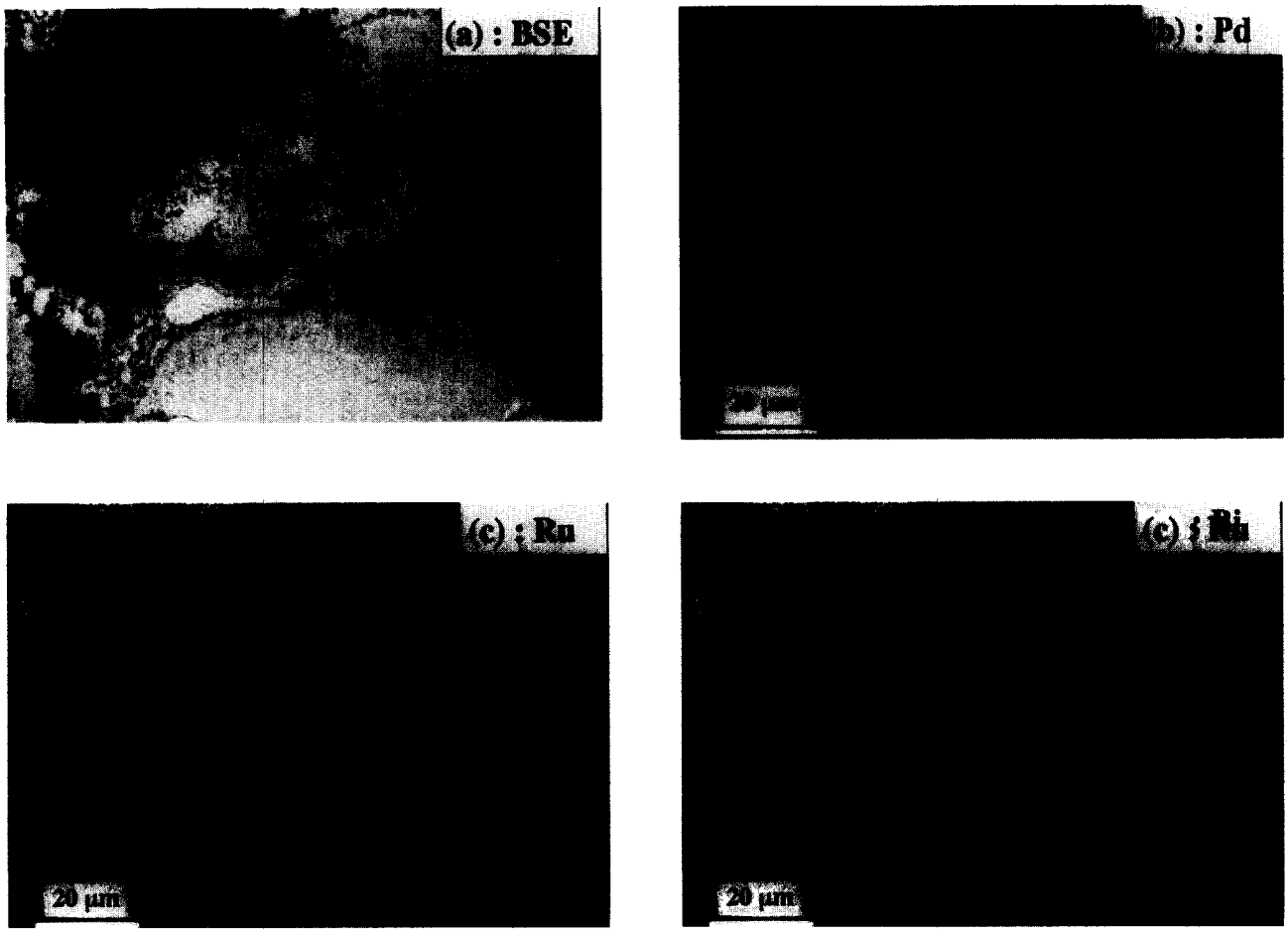

FIG. 20. Backscattered electron image (a) of uraninite grains (grey) and accumulations of Pd (b), Ru (c), and Bi (d) in the matrix.

grains. The very low $^{207}Pb/^{206}Pb$ ratio (Table 3) shows that lead corresponds to radiogenic lead from highly depleted ^{235}U. Such accumulations of native lead confirm very reducing conditions and a very low sulphur content of the environment during precipitation. On the other hand, minimum (Pb_3O_4) reflecting more oxidizing conditions has been described by Savary and Pagel (1993) as micro-inclusions of 50 to 60 μm size around uraninite crystals located at the edges of the reactor 10. Minimum is interpreted as the result of radiolysis of water which allows the formation of O_2 and H_2, hydrogen being more mobile and volatile than oxygen.

5.3. Phosphates

Different types of phosphate minerals were found in the clays and in the core of the reactors 10, 13, and 16. The most important are hydroxyapatites up to one millimeter in size. Under an optical microscope they show a zonation and contain many fluid inclusions for which thermometric data were presented in a previous section. These apatites show more or less altered edges and replacement by new crystallized Mg-chlorites suggesting that they crystallized during criticality. Isotopic analyses by thermal ionisation mass spectrometry have shown that the apatites have trapped fissiogenic nuclides such as Nd, Sm, Sr, and even low amounts of Rb (Hidaka et al., 1994a; Carpena and Sère, 1994; Bros et al., 1995). ^{235}U enrichment ($^{235}U/^{238}U$ = 0.008) has also been discovered is these apatites, giving evidence for ^{239}Pu retention (Bros et al., 1995). This suggests that apatite crystallized during the fission reaction or soon after the criticality.

In the core of the reactor 13, microcrystals of Al-phosphates are intimately associated with uraninite grains (Fig. 21). Electron microprobe analyses of these phosphate minerals (Table 7) reveal that they belong to the group of the crandallite-goyazite-florencite Al-phosphate minerals. SIMS analyses allowed an estimate of the proportion of fissiogenic elements in these minerals. The results which are reported in Table 7 indicate that most of the Zr, Ce, Nd, and Sm are of fissiogenic origin.

At Bangombé, Janeczeck and Ewing (1995a) have described Florencite-(Ce) and florencite-(La) in the clays of the reactor and in the surrounding sandstone which contains fissiogenic REEs. SIMS analyses revealed that Nd and Sm in florencite-(La) consists of approximately 33–37% fissiogenic Nd and 74–78% fissiogenic Sm and the florencite is

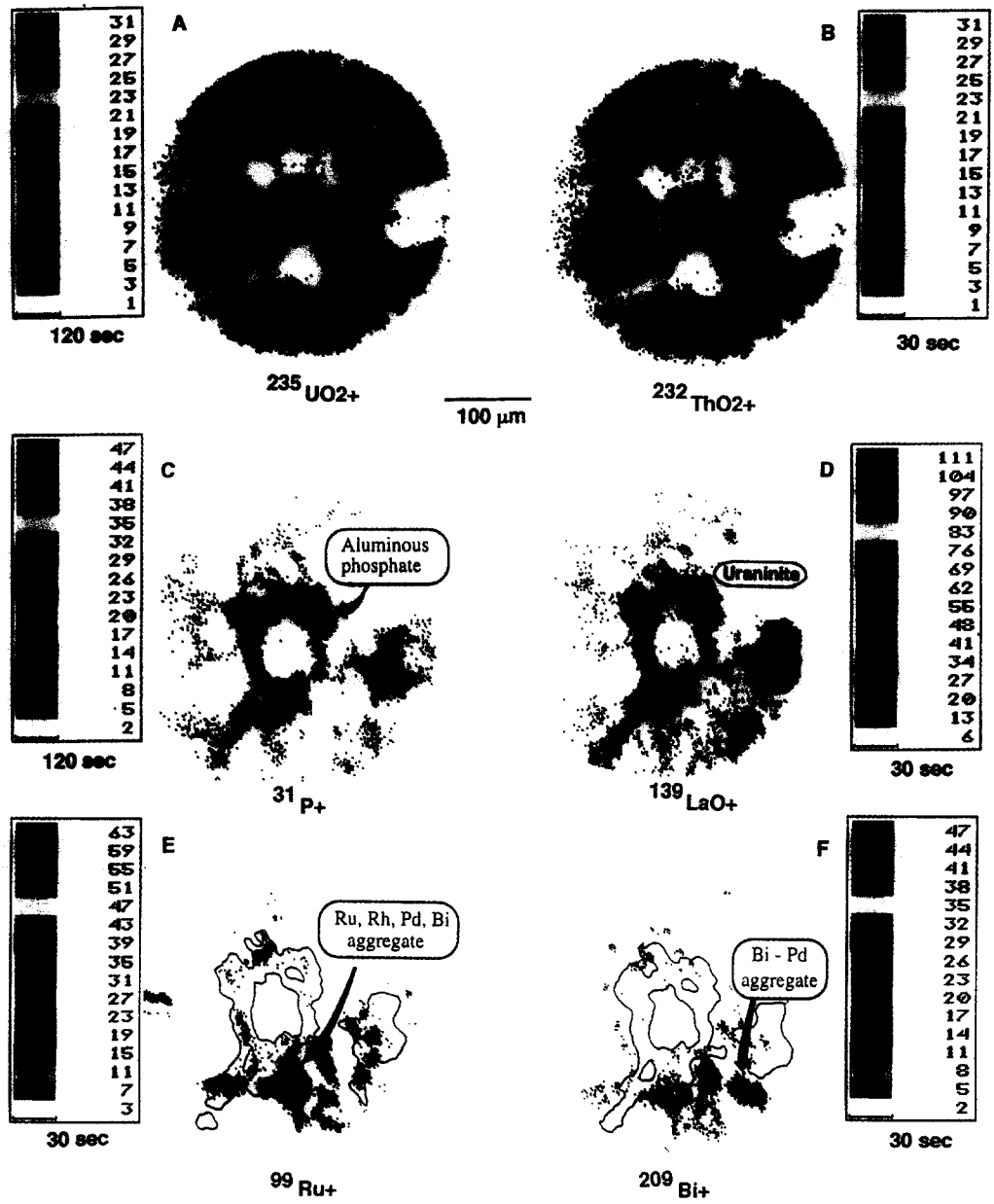

FIG. 21. Ion map of sample SD37-S2/50. Reactor 13. Distribution of U, Th, P, La, Ru, and Bi in uraninite grains, Al-phosphates minerals and metallic aggregates.

Table 6

Microprobe analyses of metallic aggregates (atomes %) in reactors 10 and 13

	Pb	Ru	Rh	Te	U	As	S	Sum.
Reactor 10 (bore hole SF29)								
2	28.22	18.12	3.75	0.62	0.61	25.11	19.44	95.87
4	14.16	31.79	6.64	0.47	3.73	35.20	3.94	95.93
Mean (5)	20.51	25.06	4.63	0.70	1.42	31.39	11.62	95.32
Reactor 13 (bore-hole SD37-S2)								
12	54.39	16.94	2.23	2.09	3.38	5.15	11.11	95.29
16	32.84	39.77	6.53	2.53	0.17	8.65	6.22	96.71
24	28.20	31.17	5.22	4.20	2.61	15.23	6.86	93.49
30	27.08	41.30	5.83	3.10	0.32	11.63	5.95	95.21
Mean (41)	38.87	33.47	4.63	2.70	0.40	8.02	7.44	95.54

The data correspond to samples showing the maximum contents and to the mean values

enriched in LREEs with respect to the bulk sample of the clays. In the sandstones some 20 cm outside the core of the reactor of Bangombé, Janeczek and Ewing (1996) have described françoisite-(Nd), $RE(UO_2)_3O(OH)(PO_4)_2 \cdot 6H_2O$ which was first (and only) discovered in the copper-cobalt deposit at Kamoto, Zaïre (Piret et al., 1988).

5.4. Clays

In the various reactors different clay minerals crystallized. Their distribution is given in Table 8 and their chemical compositions and structural formula in Table 9. The reactor 2 is characterized by various types of clay minerals which

Table 7
Aluminous hydroxy-phosphate. Reactor 13. Mean chemical (% weight of 10 analyses) and isotopic compositions

Al2O3	P2O5	SiO2	CaO	SrO	La2O3	Ce2O3	Pr2O3	Nd2O3	SmO	F	Cl
27.04	18.97	1.18	4.13	7.6	5.68	0.95	0.66	0.37	0.03	1.47	0.3

	Sr		Zr			Ce	Nd			Sm
	87/86	88/86	90/91	92/91	94/91	142/140	144/143	145/143	146/143	149/147
SD37	0.735	8.47	1.58	1.11	1.18	0.86	1.329	0.743	0.64	0.007
%Fission.	<3	0	84	84	85	>98	>98	>98	>98	100

reflect the occurrence of a high thermal gradient around the reactor during the fission reactions (Weber et al., 1975; Gauthier-Lafaye and Weber, 1978; Tchibena-Makosso, 1982; Gauthier-Lafaye, 1986; Gauthier-Lafaye et al., 1989). Fe-chlorite and the polytype 1 M of illite occur in the sediments not affected by hydrothermal alteration. The clays of the reactor are mainly made of Mg-chlorite and 2 M illite which is the high temperature polytype of illite. In these rocks, chlorite may replace the detrital biotite in ancient fine sandstones and crystallize in the matrix, whereas illite usually replace detrital quartz, now totally dissolved. In the core of the reactor, aluminous chlorite and illite of 1 Md polytype appear. These two minerals crystallized perpendicularly to the edges of the uraninite crystals suggesting that they were formed after the precipitation of the uranium oxides. We will see that isotopic data (K-Ar and oxygen isotopes) also suggest a late crystallization during their cooling, after the fission reactions stopped.

In reactor 10, illite corresponds to a minor phase, whereas Mg-chlorite and Al-chlorite are the dominant phases in the clays of the reactor and in the core, respectively. X-ray study of the Al-chlorite has shown that this mineral is a sudoïte, of which the measured unit cell parameters are given in Table 10. In the reactor of Bangombé, chlorite represents a minor phase and the clays of the reactor as well as the weathered profile are mainly made of illite (Bros et al., 1995; Eberly et al., 1995). The clay mineral characterizing the weathering of the reactors is mainly kaolinite which has been mainly found in the weathered profile of the Bangombé reactor and in some samples of reactor 2. However, this mineral corresponds always to a minor phase. In Bangombé, metahalloysite has been found in some samples of the weathered profile. This mineral, together with Fe-hydroxides, characterize a ferralitic alteration under a very wet equatorial climate (Novikoff, 1974).

Oxygen isotope compositions of the clays embedding reactor 2 (2 M-Illite, Fe and Mg-Chlorites, Al-Chlorites) revealed that they crystallized during criticality under a thermal gradient of 100°C/m (Gauthier-Lafaye et al., 1989). In the core of the reactor, however, clays crystallized after the fission reactions stopped, during the cooling stage, e.g., at diagenetic temperatures. The same was found for reactor 10 (Taieb et al., 1993).

In reactor 10 (bore-hole SF29, Fig. 7), clay minerals were extracted and size fractions smaller than 2 μm were analyzed for their uranium content, and U, Sm, Nd, Sr, and Rb isotopic compositions (Bros et al., 1993). On the same fractions, leaching experiments with 1 N HCl were also performed in order to differentiate elements incorporated in the crystallographic structure of the clays from elements adsorbed on the surface of the particles. For each sample, proportions of fissiogenic REEs were calculated. Results (Table 11) show that clay minerals located close to the top of the core of the reactor have incorporated more than 70% of Sm and Nd of fissiogenic origin (samples 624 and 625), whereas this proportion decreases to a few percent in other samples. Except for samples located at the bottom of the reactor 10 (samples 767 and 773), uranium isotopic compositions show abnormal values in both leachates and residues, reflecting mobilization and migration of depleted ^{235}U during and/or after criticality even at a few meters from the core of the reactor (3 m). One sample (768) however shows a peculiar $^{235}U/^{238}U$ ratio (0,010) with an enrichment in ^{235}U (Bros et al., 1993). This anomaly is more precisely concentrated in the solid residual phase and results from the migration of plutonium 239 ($t_{1/2}$ = 24400 g) from the core of the reactor and its trapping by clay particles before its complete decay into ^{235}U. ^{239}Pu is produced during criticality through ^{238}U resonant capture of epithermal neutrons. Rb and Sr which are fission products with relatively high fission yield have normal (natural) isotopic compositions with no fissiogenic contribution. This suggests that (1) these nuclides were not incorporated in the clay structure or (2) these elements were trapped and then exchanged after reactor operation.

Table 8
Distribution of the clay minerals in the reactors

	Reactor 2	Reactors 7 to 9	Reactor 10	Bangombé Reactor
« Normal sediments »	1M-illite Fe-Chlorite	1M- Illite Fe-Chlorite	1M-Illite Fe-Chlorite	Illite Fe-Chlorite
Weathered sediments	Kaolinite ?	-	-	Illite (Fe-Chlorite) Kaolinite metahalloysite
Clays surrounding the reactors	Mg-Chlorite 2M-Illite	Chlorite-vermiculite illite	Fe-Chlorite (1M Illite)	Illite (Mg-Chlorite)
Core of the reactor	Al-Chlorites 1Md-Illite	Al-Chlorites 1Md-Illite	Sudoite	Illite (Mg-Chlorite)

Table 9
Chemical compositions (wt %) of the clay minerals in various reactors

	SiO_2	Al_2O_3	MgO	Fe_2O_3	FeO	CaO	Na_2O	K_2O	110°C	1000°C	Total
Hosted rocks											
Illite 1Md*	48.65	28.96	2.01	4.31		0.05	0.06	7.81			91.85
Chlorite Fe-Mg*	24.94	22.96	8.57		31.10	0.02	0.04	0.04			84.00
Reactor 2											
2 M Illite : edge	46.50	31.40	2.01	1.38	1.55	0.20	0.23	8.50	1.10	5.94	98.80
1 M Illite : core*	44.25	26.98	1.91	7.65		0.15	0.10	4.12			85.20
Mg-Chlorite : core	32.00	26.40	20.10	2.31	4.40	0.20	0.05	0.24	0.48	12.10	98.28
Reactor 9											
Illite : edge + core*	43.64	30.92	0.79	6.00		0.19	0.13	4.66			86.34
Al-Chlorite : edge + core*	36.47	30.76	7.59		9.18	0.11	0.05	0.58			84.94
Reactor 10											
Fe-Chlorite : edge	34.90	27.00	10.90		12.50	0.40	0.21	0.13	2.32	14.14	100.33
Al-Chlorite : core	35.50	32.10	7.18	8.50		0.30	0.13	0.19	3.05	14.03	98.80
Bangombé											
Illite	46.20	33.2	0.50	3.20		0.10	0.26	7.14	1.30	8.71	101.30

* : Microprobe analyses

Table 10

Cell parameters of the Al-Chlorite. Reactor 10.

Sample SF29 - 82.42m. Grain size : 0.8µ

a=5.24 b=9.07 c=14.28
Beta=97.6

d A	I	h k l
14,1546	14	0 0 1
7,0773	46	0 0 2
4.7182	100	0 0 3
4,5350		0 2 0
4,5073	11	1 1 0
4,4448	8	1 1-1
4,3188	3	2 0 1
4,0163	2	1 1-2
3,5386	46	0 0 4
2,8309	12	0 0 5
2,6006	2	1 3-1
2,5970		2 0 0
2,5495	6	2 0-2
2,5395		1 3 1
2,5060	7	1 3-2
2,4964	14	2 0 1
2,4014	8	0 2 5
2,3999		1 3 2
2,3591	4	0 0 6
2,3531		1 3-3
2,3400	2	2 0 2
2,2822	3	1 1 5
2,2397	4	2 0-4
2,2390		0 4 1
2,2240	1	1 3 3
2,2224		2 2-2
2,0437	1	0 4 3
2,0382		1 3 4
2,0221	6	0 0 7
1,9980	5	1 1 6
1,9871		1 3-5
1,9729	6	2 0 4
1,9092	<1	0 4 4

d A	I	h k l
1,8739	2	2 0-6
1,8709		2 2-5
1,8120	1	1 3-6
1,8091		2 2 4
1,7989	3	2 0 5
1,7706	<1	1 1 7
1,7698		0 4 5
1,7693		0 0 8
1,7091	1	1 5-1
1,7088		2 0-7
1,7081		2 4 0
1,6914	1	1 5 1
1,6721	2	2 2 5
1,6706		3 1-3
1,6631	<1	3 1 1
1,6533	1	1 3-7
1,6527		2 4-3
1,6483	1	0 2 8
1,6482		1 5 2
1,6284	<1	2 4 2
1,6068	<1	3 2 1
1,5631	6	2 4 3
1,5615		2 0-8
1,5500		1 3 7
1,5494	2	3 1-5
1,5435	6	2 2 6
1,5125	8	2 3-8
1,5124		3 3-1
1,5117		0 6 0
1,4783	4	0 6 2
1,4764		2 2-8
1,4763		3 3 1

Table 11

Reactor 10, bore-hole SF29. Uranium content and isotopic composition, total Sm and Nd contents and their fissiogenic proportions and isotopic compositions of Sr and Rb. Clay minerals of bore-hole SF29.

Sample	U ppm	U 235/238	Sm ppm	Smf %	Nd ppm	Ndf %	Sr 86/88	Rb 85/87
765	4.25	0.007093	0.43	1.1	2.27	0		
767 L	110.3	0.007216	0.41	0.2	1.36	2.8	0.1192	
767 U	126.5	0.007228	0.29	3.1	1.75	1.7	0.1205	2.6013
767 R	19.0	0.007247	0.09	2.5	0.74	1.7	0.1204	
768 L	2.47	0.006805	0.07	0.4	0.54	2.6	0.1205	
768 U	3.34	0.007682	0.84	3.7	5.35	3.0	0.1206	2.6064
768 R	**0.83**	**0.010511**	**0.81**	**4.1**	**5.80**	**3.3**	**0.1188**	
768 R bis	0.85	0.010420						
773 L	66.9	0.007202	0.23	3.8	0.80	3.6	0.1191	
773 U	146.1	0.007226	1.75	3.1	13.26	2.2	0.1193	2.5894
773 R	93.7	0.007254	2.18	3.2	18.98	2.1	0.1194	
624	5772.8	0.006709	1.91	70.3	8.09	77.2		
625 L	53.0	0.006577	0.04	48.3	0.23	73.5		
625 U	69.1	0.006579	0.29	81.2	0.96	83.4		
625 R	16.1	0.006548	0.21	78.8	0.73	84.2		

U : untreated sample. L: leachate. R: residue.
Smf and Ndf : proportion of fissiongenic Sm and Nd respectively.
Natural 86Sr/88Sr and 85Rb/87Rb ratios are 0.1185 and 2.587 respectively.

5.5. Calcite

Calcite is mainly located in the hydraulic fracturing network which affects the clays and the core of the reactors. It corresponds to fibrous calcite with fibers oriented perpendicularly to the edges of the fractures. Some calcite may be associated with low amounts of Fe-oxides which give a red color to the mineral. In reactor 13, calcite is a common phase which occurs in every joints affecting the sandstones and the core of the reactor. Some of the calcite is also associated with the dolerite dike where it fills the joints. Sr isotopic composition of calcite have natural values suggesting that it crystallized after reactor operation (Bros, 1993).

6. CONCLUSION

The natural nuclear fission reactors of Oklo and Bangombé are located in the oldest nonmetamorphic sedimentary basin known in the world. This unusual geologic situation indicates the very improbable discovery of other fission reactors in the world and therefore make Oklo an unique geological object. The relatively simple geological history of the basin has contributed to the retention of the actinides and radionuclides in the reactors. Table 12 summarizes the behavior of these elements at Oklo and the principal phases in which they were retained. By analogy with irradiated anthropogenic uranium dioxides one can consider four types of elements depending on their behavior:

1) Fission product oxides which are soluble in the UO_2 matrix: REEs (La, Ce, Pr, Nd, Sm and Gd), Y, Nd, and Zr;
2) Fission products which are nonsoluble in the UO_2 matrix: Rb, Sr, and Ba;
3) Metallic or oxide inclusions made of Mo, Tc, Ru, Rh, Pd, and Te;

Table 12

Synthesis of the behavior of the fission products and actinides at Oklo

Behavior of fission products and actinides at Oklo								
Element	Valence	Ionic radii A	Retention					
			Core of the reactor			Clays of the reactor		
			Uraninites	Inclusions	Migration	Clays	Others	
Cs	1	1,67			■			
Rb	1	1,47			■			
Sr	2	1,12			■			
Ba	2	1,34			■			
Mo	4	0,70		■				
Tc	4	0,69		■		■		
Ru	4	0,67		■		■	?	
Rh	3	0,68		■		■	?	
Pd	2	0,80		■		■	?	
Y	3	0,92	■			■		
Nb	4	0,74	?					
Zr	4	0,79	■			■	■	
Te	4	0,70						
REE light	3	1,06-0,94	■			■	■	
Ce	4	0,92						
Pb	2	1,20						
Pb	4	0,84	■				■	
Bi	3	0,96						
Th	4	1,02	■			■	■	
U	4	0,97	■			■	■	
Np	4	0,95	?					
Pu	4	0,93	■			■	■	

■ Close relation to no relation between the minerals and the chemical elements

4) Volatile fission products: Cd, Cs, and noble gases (Xe, Kr).

At Oklo there have been two main periods of migration of radionuclides: (1) during the criticality and (2) during the time of dolerite dike intrusion. During criticality, the *P-T* conditions around the core of the reactors should have been quite similar to those we find in the primary circuit of a PWR nuclear plan: 300 to 400°C and 150–160 bars. Migration of elements was mainly due to the circulation of hydrothermal fluids which occurred around the core of the reactors and which is responsible for the alteration of the host rocks. The intrusion of the dolerite dike corresponds to a major extensional event in the basin. This tectonic event reopened ancient faults and fractures allowing new migrations of fluids in the basin. This event is mainly responsible for a massive migration of radiogenic lead and of the elements forming metallic and oxide inclusions (platinum metals, Mo, Te) in uranium oxides. At Bangombé, the present weathering of the reactor under a wet equatorial climate also contributes to the redistribution of uranium and of the end-member fission products into the surrounding rocks and soils.

The analogy between the Oklo reactors and the man-made nuclear waste disposal systems is mainly in that Oklo is the only occurrence in the world were actinides and fission products have been in a geological environment for a very long period. The purpose of this study was to determine which are the main geological, mineralogical, and geochemical parameters which either allow the retention or the migration of the actinides and radionuclides in a geological system. Presently, we suggest that three factors controlled the preservation of the reactors. The first one is the geological stability of the Franceville basin. The second is the low permeability of the rocks enclosing the reactors. This is mainly due to the presence of clay layers enclosing the core of the reactors and due to the closure of the porosity and permeability of the surrounding sandstones during the diagenesis of the basin. At present, the permeability of the sandstone in the Oklo deposits is close to zero. Finally, the third factor is the preservation of the uraninites allowing the retention of the fission products which are soluble within the UO_2 structure. The preservation of uranium dioxides is favored by the reducing conditions in the reactors which prevail due to the presence of organic matter (Nagy et al., 1991, 1993). The importance of clay and phosphate minerals for the retention of actinides and fission products has also been shown, and this demonstrates the importance of secondary barrier in the confinement of radionuclides.

Acknowledgments—This manuscript benefited greatly from official reviews by H. Hidaka and R. Loss and from discussions and comments of B. Nagy, P. Stille, R. Bros, and K. A. Jensen. A review by R. Ewing has made important improvement on the initial manuscript. This work was supported by the French Commissariat à l'Energie Atomique (IPSN) and by the European programme «Oklo-Natural analogues» (Contract CCE n°F112W-CT91-0071). The authors want to thank the Compagnie de Mines d'Uranium (COMUF) for their help in Gabon and during the mining works of the reactors.

Editorial handling: R. A. Schmitt

REFERENCES

Bodu R., Bouzigues H., Morin N., and Pfiffelmann J. P. (1972) Sur l'existence d'anomalies isotopiques rencontrées dans l'uranium du Gabon. *C. R. Acad. Sci. Paris* **275,** 1731–1734.

Bonhomme M., Gauthier-Lafaye F., and Weber F. (1982) An example of Lower Proterozoic sediments: the Francevillian in Gabon. *Precambrian Res.* **18,** 87–102.

Brookins D. G. (1975) Fossil reactor's history is probed. *Geotimes* (Oct. 1975), 14–18.

Bros R. (1993) Géochimie isotopique (Sm-Nd, Rb-Sr, K-Ar, U) des argiles du bassin Protérozoïque de Franceville et des réacteurs d'Oklo (Gabon). Ph.D. dissertation, Univ. Strasbourg.

Bros R., Stille P., Gauthier-Lafaye F., Weber F., and Clauer N. (1992) Sm-Nd isotopic dating of Proterozoic clay material: An example from Francevillian sedimentary Series, Gabon. *Earth Planet. Sci. Lett.* **113,** 207–218.

Bros R., Turpin L., Gauthier-Lafaye F., Holliger Ph., and Stille P. (1993) Occurrence of naturally enriched 235 uranium: implications for Pu behaviour in natural environments. *Geochim. Cosmichim. Acta* **57,** 1351–1356.

Bros R., Gauthier-Lafaye F., Larqué P., Samuel J., and Stille P. (1994) Mobility of uranium, thorium and lanthanides around the Banghombé natural nuclear reactor (Gabon). *Proc. XVIII International Symposium on the Scientific Basis for Nuclear Waste Management* (ed. R. Ewing), pp. 1187–1194.

Bros R., Carpena J., Sere V., and Beltritti A. (1996) Occurrence of Pu and fissiogenic rare earth elements in hydrothermal apatites from the fossil natural nuclear reactor 16 of Oklo (Gabon). *Proc. Migration 95, Radiochim. Acta* **74,** 277–282.

Carpena J. and Sère V. (1994) Les apatites néoformées lors des réactions nucléaires dans les zones 10 et 16 d'Oklo. *15e Réunion des Sciences de la Terre, Nancy 114* (abstr.).

Cathelinau M., Boiron M., Holliger P., and Poty B. (1990) Metallogenesis of the French part of the Variscan orogen. Part II: time-space relationships between U, Au and Sn-W ore deposition and geodynamic events—mineralogical and U-Pb data. *Tectonophysics* **177,** 59–79.

Cortial F., Gauthier-Lafaye F., Oberlin A., Lacrampe-Couloume G., and Weber F. (1990) Characterization of organic matter associated with uranium deposits in the Francevillian Formation of Gabon (Lower Proterozoic). *Org. Geochem.* **15,** 73–85.

Curtis D., Benjamin T., Gancarz A., Loss R., Rosman K., De Laeter J., Demore J. E., and Maek W. J. (1989) Fission product retention in the Oklo natural fission reactors. *Appl. Geochem.* **4,** 49–62.

Dahlkamp F. J. (1993) *Uranium Ore Deposits.* Springer-Verlag.

De Laeter J. R. and Rosman K. J. R. (1975) Cumulative fission yields of cadmium in Oklo samples. *Proc. The Oklo Phenomenon,* pp. 425–436. IAEA.

Devillers C., Ruffenach J. C., Menes J., Lucas M., Hagemann R., and Nief G. (1975) Age de la mineralisation de l'uranium et date de la réaction nucléaire. *Proc. The Oklo Phenomenon,* pp. 293–302. IAEA.

Dran J. C., Durand J. P., Langevin Y., Maurette M., and Petit J. C. (1978) Contribution of radiation damage studies to the understanding of the Oklo phenomenon. *Proc. The natural Fission Reactors,* pp. 375–388. IAEA.

Dubessy J., Pagel M., Beny J. M., Christensen H., Bernard H., Kosztolanyi C., and Poty B. (1988) Radiolysis evidence by H_2-O_2 and H_2-bearing fluid inclusions in three uranium deposits. *Geochim. Cosmochim. Acta* **52,** 1155–1167.

Eberly P., Janeczek J., and Ewing R. (1994) Petrographic analysis of samples from the uranium deposit at Oklo, republic of Gabon. *Radiochim. Acta* **66/67,** 445–461.

Eberly P., Janeczek, and Ewing R. (1995) Precipitation of uraninite in chlorite-bearing veins of the hydrothermal alteration zone (argile de pile) of the natural nuclear reactor at Bangomné, republic of Gabon. *Proc. XVIII International Symposium on the Scientific Basis for Nuclear Waste Management* (ed. R. Ewing), pp. 1195–1202.

Gancarz A. J. (1978) U-Pb age (2.05×10^9 years) of the Oklo

uranium deposit. *Proc. The natural Fission Reactors,* pp. 513–520. IAEA.

Gancarz A., Cowan G., Curtis D., and Maek W. (1980) 99Tc, Pb, and Ru migrations around the Oklo natural fission reactors. *Scientific Basis For Nuclear Waste Management* **2,** 601–608.

Gauthier-Lafaye F. (1978) Suivi géologique de l'exploitation des réacteurs naturels d'Oklo. *Proc. The natural Fission Reactors,* pp. 75–130. IAEA.

Gauthier-Lafaye F. (1986) Les gisements d'uranium du Gabon et les réacteurs d'Oklo. Modèle métallogénique de gites à fortes teneurs du Protérozoique inférieur. *Mém. Sciences Géologiques* **78.**

Gauthier-Lafaye F. (1995) Géologie des réacteurs. Etude des épontes et des transferts anciens. *Repport CEA-CEE. Contrat CCE n°F112W-CT91-0071.*

Gauthier-Lafaye F. and Weber F. (1978) Etudes minéralogiques et pétrographiques effectuées à Strasbourg sur les réacteurs naturels d'Oklo. *Proc. The natural Fission Reactors,* pp. 199–227. IAEA.

Gauthier-Lafaye F. and Weber F. (1981) Les concentration uranifères du Francevillien du Gabon: leur association avec des gîtes à hydrocarbures fossiles du Protérozoïque inférieur. *C. R. Acad. Sci. Paris* **292,** 69–74.

Gauthier-Lafaye F. and Weber F. (1988) Le mécanisme de la fracturation hydraulique dans la métallogenèse de l'uranium en série sédimentaire. L'exemple du gisement d'Oklo, Gabon. *Documents du BRGM* **158,** 445–465.

Gauthier-Lafaye F. and Weber F. (1989) The Francevillian (Lower Proterozoic) uranium ore deposits of Gabon. *Econ. Geol.* **84,** 2267–2285.

Gauthier-Lafaye F., Weber F., Naudet R., Pfiffelmann J. P., Chauvet R., Michel B., and Reboul J. C. (1979) Le gisement d'Oko et ses réacteurs de fission naturels. *Proc. Uranium in the Pine Creek Geosyncline,* pp. 663–673. IAEA.

Gauthier-Lafaye F., Weber F., and Ohmoto H. (1989) Natural fission reactors of Oklo. *Econ. Geol.* **84,** 2286–2295.

Geoffroy J. (1975) Etude microscopique des minerais uranifères d'Oklo. *Proc. The Oklo Phenomenon,* pp. 133–152. IAEA.

Hagemann R. and Roth E. (1978) Relevance of the studies of the Oklo nuclear reactors to the storage of radioactive wastes. *Radiochim. Acta* **25,** 241–247.

Hagemann R., Lucas M., Nief G., and Roth E. (1974) Mesures isotopiques du rubidium et du strontium et essais de mesure de l'âge de la minéralisation de l'uranium du réacteur naturel d'Oklo. *Earth Planet. Sci. Lett.* **23,** 170–176.

Hagemann R., Devillers C., Lucas M., Lecomte T., and Ruffenach J. C. (1975) Estimation de la durée de la réaction. Limitation par les données neutroniques. *Proc. The Oklo Phenomenon,* pp. 415–422. IAEA.

Hidaka H. (1995) Isotopic evidence for the retention of fissiogenic nuclides in and around reactor zones. *Nuclear Sience and Technology-Oklo Working Group, EUR 16704,* 47–58.

Hidaka H. and Masuda A. (1988) Nuclide analyses of rare earth elements of the Oklo uranium ore samples: a new method to estimate the neutron fluence. *Earth Planet. Sci. Lett.* **88,** 330–336.

Hidaka H., Masuda A., Fujii I., and Shimizu H. (1988) Abundance of fissiogenic and pre-reactor natural rare-earth elements in a uranium ore sample from Oklo. *Geochem. J.* **22,** 47–54.

Hidaka H., Konishi T., and Masuda A. (1992) Reconstruction of Cumulative Fission Yield Curve and Geochemical Behaviors of Fissiogenic Nuclides in the Oklo Natural Reactors. *Geochem. J.* **26,** 227–239.

Hidaka H., Holliger P., and Masuda A. (1993a). Evidence of fissiogenic Cs estimated from Ba isotopic deviations in a Oklo natural reactor zone. *Earth Planet. Sci. Lett.* **114,** 391–396.

Hidaka H., Shinotsuka K., and Holliger P. (1993b) Geochemical behaviour of 99Tc in the Oklo natural fission reactors. *Radiochim. Acta* **63,** 19–22.

Hidaka H., Sugiyama T., Ebihara M., and Holliger P. (1994a) Isotopic evidence for the retention of 90Sr inferred from excess 90Zr in the Oklo natural fission reactors: implication for geochemical behaviour of fissiogenic Rb, Sr, Cs and Ba. *Earth Planet. Sci. Lett.* **122,** 173–182.

Hidaka H., Takahashi K., and Holliger P. (1994b) Migration of fission products into micro-minerals of the Oklo natural reactors. *Radiochim. Acta* **66/67,** 463–468.

Holliger P. and Devillers C. (1981) Contribution à l'étude de la température dans les réacteurs fossiles d'Oklo par la mesure du rapport isotopique de Lutétium. *Earth Planet. Sci. Lett.* **52,** 76–84.

Holliger P. (1992) Les nouvelles zones de réaction d'Oklo: datation U-Pb et caractérisation in-situ des produits de fission à l'analyseur ionique. *Programme "Oklo-Analogues Naturels," Note technique CEN Grenoble DEM n°01/92.* Commissariat à l'Energie Atomique.

Holliger P. (1993) SIMS studies on the Oklo natural fission reactors *Proc. SIMS IX Conference, Yokohama,* (Invited lecture) pp. 8–12.

Holliger P. (1995) Terme source: caractérisation isotopique, paramètres nucléaires et modélisation. *Repport CCE n°F112W-CT91-0071. Programme Oklo–Analogues Naturels.*

Holliger P., Devillers C., and Retali G. (1978) Evaluation des temperatures neutroniques dans les zones de réaction d'Oklo par l'étude des rapports isotopiques 176Lu/175Lu et 156Gd/155Gd. *Proc. The natural Fission Reactors,* pp. 553–565. IAEA.

Janeczek J. and Ewing R. (1992) Dissolution and alteration of uraninite under reducing conditions. *J. Nucl. Materials* **190,** 157–173.

Janeczek J. and Ewing R. (1995a) Florencite-(La) with fissiogenic REE from a natural fission reactor at Bagombé, Gabon. *Amer. Mineral.* (in press).

Janeczek J. and Ewing R. C. (1995b) Mechanisms of lead release from uraninite in the natural fission reactors in Gabon. *Geochim. Cosmochim. Acta* **59,** 1917–1931.

Janeczek J. and Ewing R. (1996) Phosphatian coffinite with rare earth elements and françoisite-(Ce, Nd) from sandstone beneath a natural fission reactor at Bangmbé, Gabon. *Mineral. Mag.* **60,** 665–669.

Kleykamp K. (1985) The chemical state of fission products in oxide fuels. *J. Nucl. Materials* **131,** 221–246.

Lancelot J. R., Vitrac A., and Allègre C. J. (1975) The Oklo natural reactor: Age and evolution studies by U-Pb and Rb-Sr systematics. *Earth Planet. Sci. Lett.* **25,** 189–196.

Loss R. D., Rosman K. J. R., and de Laeter J. R. (1984) Transport of symmetric mass region fission products at the Oklo natural reactors. *Earth Planet. Sci. Lett.* **68,** 240–248.

Loss R. D., DeLaeter J. R., Rosman K. J. R., Benjamin T. M., Curtis D. B., Gancarz A., Delmore J. E., and Maek W. J. (1988) The Oklo natural reactors: cumulative fission yields and nuclear characteristics of reactor Zone 9. *Earth Planet. Sci. Lett.* **89,** 193–206.

Loss R. D., Rosman K. J. R., De Laeter J. R., and Curtis D. B. (1989) Fission product retentivity in peripheral rocks at the Oklo natural fission reactors, Gabon. *Chem. Geol.* **76,** 71–84.

Nagy B., Gauthier-Lafaye F., Holliger Ph., Davis D. W., Mossman D. J., Leventhal J. S., Rigali M., and Parnell J. (1991) Role of organic matter in containment of uranium and fissiogenic isotopes at the Oklo natural reactors. *Nature* **354,** 472–475.

Nagy B., Gauthier-Lafaye F., Holliger P., Mossman D., Leventhal J., and Rigali M. (1993) Role of organic matter in the proterozoic Oklo natural fission reactors, Gabon, Africa. *Geology* **21,** 655–658.

Naudet R. (1975) Mécanismes de régulation des réactions nucléaires. *Proc. The Oklo Phenomenon,* pp. 589–600. IAEA.

Naudet R. (1976) The Oklo nuclear reactors: 1800 million years ago. *Interdisciplinary Science Reviews* **1,** 72–84.

Naudet R. (1978) Etude paramétrique de la criticité des réacteurs naturels. *Proc. The natural Fission Reactors,* pp. 589–600. IAEA.

Naudet R. (1991) *Oklo: des réacteurs nucléaires fossiles.* Collection du Commissariat à l'Energie Atomique Paris.

Naudet R. and Renson C. (1975) Résultats des analyses systématiques de teneurs isotopiques de l'uranium. *Proc. The Oklo Phenomenon,* pp. 265–288. IAEA.

Neuilly M. and Naudet R. (1975) Etude de la distribution des flu-

ences dans les réacteurs naturels d'Oklo, par analyse isotopique des terres rares. *Proc. The Oklo Phenomenon,* pp. 541–556. IAEA.

Neuilly M., Bussac J., Frejacques C., Nief G., Vendryes G., and Yvon J. (1972) Sur l'existence dans un passé reculé d'une réaction en chaîne naturelle de fission, dans le gisement d'uranium d'Oklo (Gabon). *C.R. Acad. Sci. Paris* **275,** 1847–1849.

Novikoff A. (1974) L'altération des roches dans le massif du Chaillu (République Populaire du Congo). Formation et évolution des argiles en zone ferralitique. Ph.D. dissertation, Univ. Louis Pasteur.

Openshaw R., Pagel M., and Poty B. (1978) Phases fluides contemporaines de la diagenèse des grès, des mouvements tectoniques et du fonctionnement des réacteurs nucléaires d'Oklo (Gabon). *Proc. The natural Fission Reactors,* pp. 265–296. IAEA.

Piret P., Deliens M., and Piret-Meunier J. (1988) La françoisite-(Nd), nouveau phosphate d'uranyle et de terres rares; propriétés et structure cristalline. *Bull. Minéral.* **11,** 443–449.

Reuss P. (1975) Modèles d'évolution de l'uranium et des produits de fission. *Proc. The Oklo Phenomenon,* pp. 565–572. IAEA.

Royer J-J., Gerard B., and Le Carlier de Veslud C. (1995) Modeling heat and fluid transfers during natural nuclear reaction in the Oklo uranium deposit (Gabon). *Nuclear Science and Technology-Oklo Working Group, EUR 16704,* pp. 75–101.

Ruffenach J. C. (1978) Etude des migrations de l'uranium et des terres rares sur une carotte de sondage et application à la détermination de la date des réactions nicléaires. *Proc. The natural Fission Reactors,* pp. 441–471. IAEA.

Ruffenach J. C. (1979) Les réacteurs nucléaires naturels d'Oklo. Paramètres neutroniques, date et durée de fonctionnement, migrations de l'uranium et des produits de fission. Ph.D. dissertation, Univ. Paris VII.

Savary V. and Pagel M. (1993) Redox conditions and thermal history in reactors 10 and 16. *Nuclear Sciences and Technology-Oklo Working Group, Brussel, Report EUR 16098,* pp. 51–62.

Savary V., Pagel M., Pironon J., Holliger P., and Gauthier-Lafaye F. (1993) Redox conditions in the Oklo nuclear reactor zones. *Terra* **5,** 510 (abstr.).

Stille P., Gauthier-Lafaye F., and Bros R. (1993) The neodynium isotope system as a tool for petroleum exploration. *Geochim. Cosmochim. Acta* **57,** 4521–4525.

Shukolyukov Y. A., Meshik A. P., Moshanskaya N. G., Dang Vu Minh, Ramendik G. I., Tyurin D. A., and Makarov V. A. (1985) Isotope anomalies in the natural nuclear reactors at the Oklo uranium deposit, Republic of Gabon, Africa. *Geokhimiya* **11,** 1630–1644.

Taieb R., Gauthier-Lafaye F., Sharp Z. D., and Jakubick A. T. (1993) O and H isotope compositions of hydrothermal chlorites from Oklo natural reactors, Gabon. *Terra* **5,** 658 (abstr.).

Tchibena-Makosso J-P. (1982) Effets sur l'encaissant des réctions de fission naturelles d'Oklo (République Gabonaise). Evolution minéralogique des phyllosilicates et bilans géochimiques. Ph.D. dissertation, Univ. Louis Pasteur.

Vanderbroucke M., Rouzaud J. N., and Oberlin A. (1978) Etude géochimique de la matière organique insoluble (kérogène) du minerai uranifère d'Oklo et de schistes apparentés du Francevillien. *Proc. The natural Fission Reactors,* pp. 307–332. IAEA.

Weber F. (1968) Une série précambrienne du Gabon: le Francevillien. Sédimentologie, géochimie et relation avec les gîtes minéraux associés. *Mém. Serv. Carte Géol. Als. Lorr.* **28.**

Weber F., Geffroy J., and Le Mercier M. (1975) Synthèse des études minéralogiques et pétrographiques des minerais d'Oklo, et de leurs gangues et des roches encaissantes. *Proc. The Oklo Phenomenon,* pp. 173–192. IAEA.

Winkler H. G. F. (1976) *Petrogenesis of Metamorphic Rocks.* Springer-Verlag.